Cell News

Newsletter of the German Society for Cell Biology
full electronic version
Volume 47, 2 2021

DGZ Prize Winners 2021

Discovering the subcellular dynamics of life.

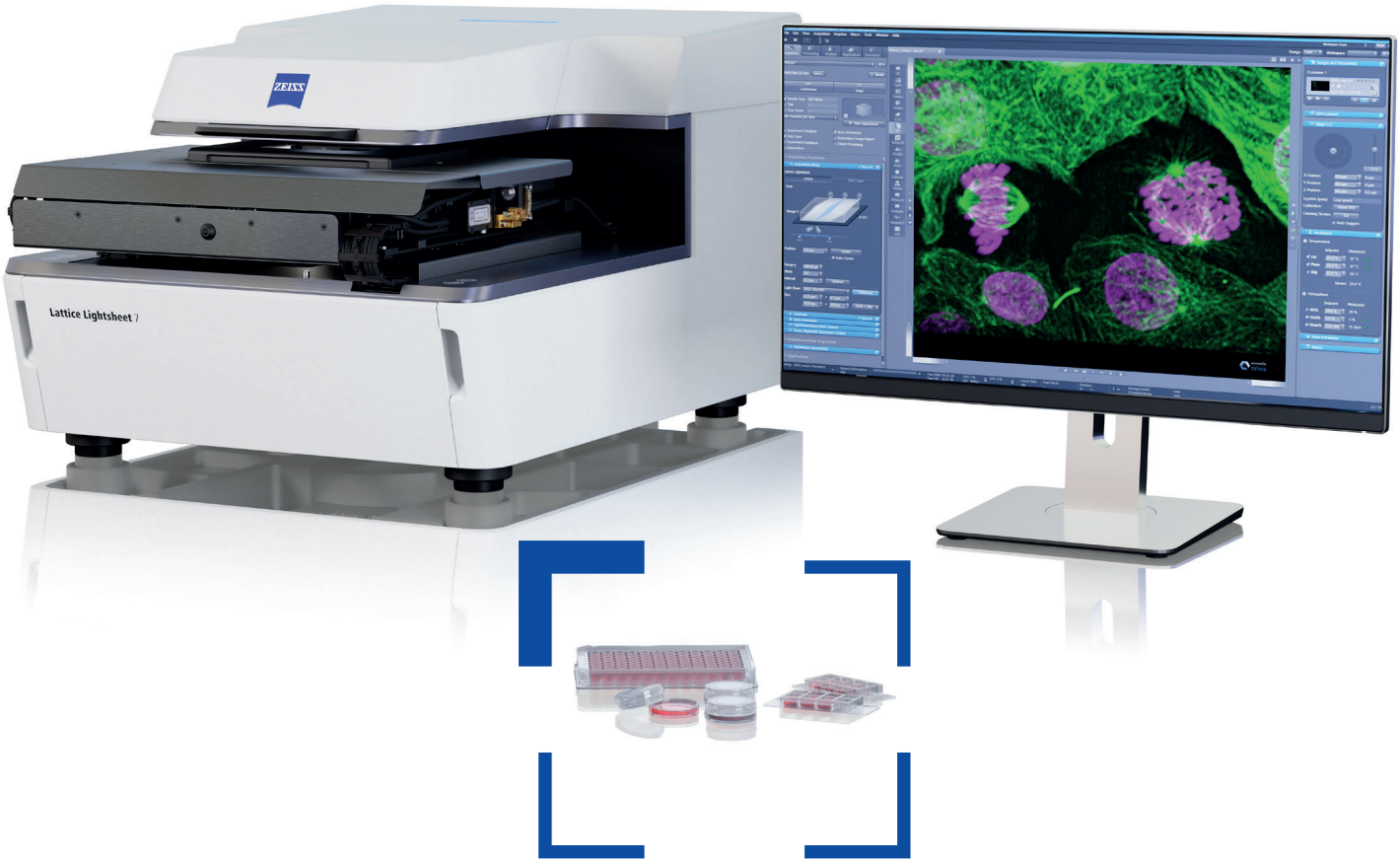

Long-term volumetric imaging of living cells

ZEISS Lattice Lightsheet 7 makes light sheet fluorescence microscopy available for live cell imaging at subcellular resolution – while also allowing you to use your standard sample carriers. Volumetric imaging of subcellular structures and dynamics over hours and days becomes available to everyone. Discover the dynamics of life in unprecedented depth of detail – with the ease you never imagined possible!

zeiss.com/lattice-lightsheet

ZEISS

Seeing beyond

CONTENT

Office:
Sabine Reichel-Klingmann
c/o Deutsches Krebsforschungs-zentrum (DKFZ)
Im Neuenheimer Feld 280
69120 Heidelberg
Tel.: 0 62 21 / 42-34 51
Fax: 0 62 21 / 42-34 52
E-Mail: dgz@dkfz.de
Internet: www.zellbiologie.de

Cover Image: DGZ Prize Winners 2021: All award presentations can be found on the DGZ homepage (https://zellbiologie.de/wissenschaftspreise/) and in this issue of Cell News several of the winners give us some additional insights into their work.

Dear members and friends of the German Society for Cell Biology,

As we all know, even after two years in the grip of the pandemic, the battle against the virus is far from over. And science is positioned right in the middle of fault lines that have opened up in societies around the world. In a global effort of unprecedented scope and speed, scientists have uncovered the molecular mechanisms of COVID infections and developed potent vaccines to protect from it. The ensuing broad interest in medical and biological research has then been faced with equally widespread backlash, not only against political restrictions but also against those same vaccines and the experts who promote them. This backlash was influential enough to prevent a sufficiently high rate of vaccination here in Germany and other countries.

For a long time, many scientists have defined their role in society to only present "hard facts" from their research but not to actively engage as what we might call "public intellectuals". We clearly cannot afford such luxury any longer. As scientists and scientific society we are all called upon to actively communicate in our respective circles and outlets in order to help increase vaccination acceptance – and to combat fake news, whether born out of intent or ignorance.

One option surely is to strengthen the voice of cell biologists and we hope that our common platform here will continue to grow.

Due to the continued restrictions for most events, the DGZ has shifted its activities to online formats. Despite the inherent difficulties in personal online interactions these formats offer greater ease of access and wider geographic reach and hence also promise to expand our visibility. The positive feedback we received in recent months is definitely encouraging.

Since our last Cell News issue in May things at the DGZ have been quite busy:

- **Our International Meeting** "Life in between – The cell biology of interfaces" was held in the virtual environment of the Münster Castle from 27th-29th of September 2021. The meeting showcased various local and national research consortia working on cellular interfaces as well as the work performed at the mechanobiology institute (MBI) in Singapore in dedicated sessions. All presentations, including the 23 selected short talks from submitted abstracts, were of exceptional quality and illustrated the cutting edge and highly interdisciplinary work performed by cell biologists in all areas of life science. Sponsored by the European Journal of Cell Biology, we were able to award prizes to the 3 best short presentations by Pia Brinkert, Jacopo di Russo and Adrian Hodel. All talks were available for viewing to registered participants for 4 weeks after the meeting.
- Our revamped **DGZ web page** is still in development but should be up at the start of 2022. In addition to the existing content on meetings, news, member meetings and prizes it will feature an interactive map to facilitate the search for cell biology groups across Germany and protected access to our members to advertise and administer their own personal details, job offers and press releases. Since July this year we also have an online presence on **Twitter (@DGZ_2021)**. Please follow us to receive all news and announcements and share in current scientific trends. And please help share our news!
- To increase opportunities for networking and scientific exchange in our society we have decided to follow the cell's example and compartmentalize. We established **twelve working groups (WG)** that will focus on specific scientific themes. Each WG will be coordinated by two speakers and will present their topic to a larger audience in a monthly focus workshop that features presentations by scientists of different career stages. In the coming weeks all members will be asked to join one or more of these WG that represent their respective research focus.
- **Scientific awards 2021:** Thanks to the generous sponsorship by ibidi we could reintroduce the Walther Flemming Award to honor groundbreaking research establishing the independence of young scientists. Together with the other four awards, our prizes cover the whole range of scientific career stages and were again awarded in an online ceremony on November 18th. Katharina Scheibner from the Helmholtz Center Munich received the Nikon Young Scientist Award and Isidora Paredes Ugarte from the ECAS in Heidelberg is the recipient of the Werner Risau Prize. Matteo Allegretti received the Walther Flemming Award and Leo Kurian from the CMMC and CECAD in Cologne is the recipient of the BINDER Innovation Prize. Finally, Frank Bradke from the DZNE in Bonn presented a beautiful roundup of his research into neuronal growth and regeneration in the Carl Zeiss Lecture 2021. All award presentations can be found on the DGZ homepage (https://zellbiologie.de/wissenschaftspreise/) and in this issue of Cell News several of the winners give us some additional insights into their work.

We know by now that a return to pre-pandemic conditions will not happen anytime soon. In the meantime we will aim to use all available tools at our disposal to strengthen collaborations within the cell biology community and offer additional services to our members.

Please don't hesitate to let us know your thoughts and especially criticism on our activities.

Stay safe and join us in shaping the future of cell biology in Germany.

The DGZ!

DGZ Mitgliederversammlung 2021

Liebe Mitglieder der Deutschen Gesellschaft für Zellbiologie,

Wir laden Sie ein zur diesjährigen Mitgliederversammlung der DGZ,
die am **9. Dezember 2021, 12.30 Uhr – 14.00 Uhr, online über zoom** stattfinden wird.
Die Meeting ID und das Passwort werden allen Mitgliedern rechtzeitig per email zugeschickt.

Tagesordnung:

1. Bestätigung des Protokolls der letzten Sitzung
2. Jahresbericht des Präsidenten mit anschließender Diskussion
3. Geschäfts- und Kassenbericht über das abgelaufene Kalenderjahr
4. Bericht der Rechnungsprüfer
5. Entlastung des Vorstandes
6. Genehmigung des Budgets und Festsetzung des jährlichen Mitgliederbeitrages
7. Sonstiges

DGZ Member Meeting 2021

Dear Members of the German Society for Cell Biology,

We would like to invite you to this years' member meeting of the DGZ, which is going to take place on **December 9, 2021, 12:30 h – 14:00 h, online via zoom**. The meeting ID and password will be communicated via individual email to all members in due time.

Agenda:

1. Confirmation of the minutes of the last meeting
2. Annual report of the president with discussion
3. Report on finances of the past calendar year
4. Auditors' report
5. Discharge of the board
6. Budget approval and designation of membership fees
7. Other items

Walther Flemming Award:

Architecture of the nuclear pore complex in different cellular contexts

Matteo Allegretti

Introduction

The nuclear pore complex (NPC) is a huge membrane protein complex (60MDa in S. cerevisiae) which is essential to eukaryotic life. Its function is to allow the regulated transport of molecules bigger than 40kDa in and out of the nuclear compartment (1). It consists of around 600 proteins in S. cerevisiae which are called Nups or nucleoporins and are arranged in three scaffold rings with a pseudo 8-fold symmetry. The inner ring sits at the fusion plane between the inner and the outer nuclear membrane, while the cytoplasmic and the nucleoplasmic rings are placed in their respective side of the nucleus, facing the cytoplasm or the nuclear interior. Y-complexes are multiprotein complexes which link the outer rings (cytoplasmic and nucleoplasmic) to the respective nuclear membrane (2).
The aim of my postdoctoral work was to build a pseudoatomic models of the architecture of the NPC in the cellular context and to investigate how such architecture would dynamically change according to environmental stimuli.

Methods and Results

To reach such goals I teamed up with Dr. Christian Zimmerli (EMBL) and established a pipeline for in cell structural biology together with Julia Mahamid's group at EMBL. This pipeline starts with cell culture and perturbation, it continues with cell vitrification, cryo-Focused Ion Beam milling, electron cryo tomography and subtomogram averaging. Cryo-Focused Ion Beam milling allows to cut 150-250 nm slices of the cell of interest to make it transparent to an electron beam to perform electron cryo tomography (3). After this task NPCs are selected from 3D tomographic volumes and averaged using subtomogram averaging (4). Finally, in collaboration with Jan Kosinski's lab (EMBL) we performed integrative modelling, meaning we use all the available high-resolution structures and prior information from cross-linking mass spectrometry and biochemistry to create a pseudo-atomic model of the NPC (5) as it is in the cell (Figure 1).

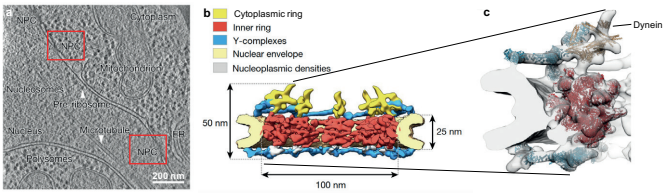

Figure 1: In cell structural biology. a) Cryo tomographic slice showing a S. cerevisiae cell in division with its macromolecular context. ER is endoplasmic reticulum. b) Subtomogram average of the nuclear pore complex in the cell with the segmentation of the main scaffold rings and nuclear membrane. The average is cut in half along the central axis. c) Integrative modelling of one of the eight asymmetric units of the NPC with X-ray models fitted. CR and NR Y-complex are depicted as blue ribbons, the integrative model of a portion of the cytoplasmic ring is shown as yellow ribbons and the refined inner ring as red ribbons. The allocated density of the NPC in the cellular context is in grey. Figure adapted from reference 7.

S. cerevisiae NPC architecture in the cell and snapshots of its turnover

We solve the structure of S. cerevisiae nuclear pore in the cellular context and found out being 20nm wider than a previous structure from purified NPCs (6) showing a stretched conformation of the Y-complexes (7). We could reveal the anchor point and the orientation of the nucleoplasmic ring including the basked rod and the organization of the cytoplasmic ring proteins with a dynein arm pointing towards the cytoplasm (7). We could solve the structure of the NPC from a Nup116 knock-out strain and localize the position of this protein at the connection point between the inner and the cytoplasmic ring (7). This Nup is essential for mRNA export, ribosomal biogenesis and a correct assembly of the NPC and it was known that the knock-out strain at the not-permissive T of 37°C would form aberration at the nuclear envelope called herniations (8). Those are bleb-like structures which involve the two nuclear membranes and are a landmark of neurodegenerative diseases (9). I used this *S. cerevisiae* knock-out strain to solve the structure at the base of such blebs and found out the presence of an NPC missing the cytoplasmic ring but retaining the inner and nucleoplasmic ring (Figure 2). Using high-throughput electron tomography in plastic sections at 5h and 24h time points, we found out that such herniae accumulate in time while the number of normal-looking NPCs decreases with time. We hypothesize that the herniae come from an unsuccessful assembly of the NPC where the two nuclear membranes fail to fuse and the cytoplasmic ring fails to integrate (Figure 2). As a physiological consequence we notice that the nuclear volume increases with time and the cell dyes in a few generations.

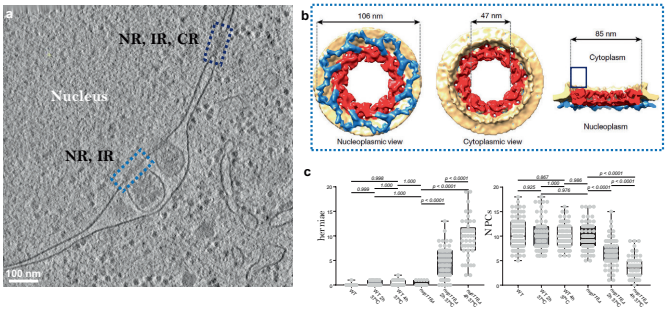

Figure 2: Nuclear envelope herniae. a) Cryo tomographic slice of the nucleus of Nup116 knock-out strain shifted to 37°C for 4h showing blebs in the nuclear envelope. NR is nucleoplasmic ring, IR is inner ring, CR is cytoplasmic ring. b) Subtomogram average of the density at the basis of the nuclear envelope bleb shows an NPC owning only the IR (red) and NR Y-complexes (blue), but missing the CR. c) Quantification of number of NPCs and herniae from 300nm tomographic volumes of S. cerevisiae cells obtained from plastic sections. Herniae accumulate with time while NPCs decrease. Figure adapted from reference 7.

At that time the group of Boris Pfander with Florian Wilfling and Chia-Wei Lee (Max Planck Institute of Biochemistry) found out that scaffold Nups are degraded by the autophagy machinery using an autophagic receptor in the cytoplasmic ring of the NPC (10). In collaboration with their group we could solve the ultrastructural pathway of such degradation using correlative light and electron microscopy and electron tomography. The autophagic receptor sits at the tip of the cytoplasmic ring's dynein arm and it is exposed to the cytoplasm. Nitrogen starvation allows to recruit Atg8 (the main autophagic protein in *S. cerevisiae*) at high abundance in the cytoplasm and Atg8 would interact with Nup159 in the cytoplasmic ring. We use a split-Venus fluorescence assay to visualize such interaction that appears as a bright spot in light microscopy. We could correlate such fluorescent spot to an electron microscopy volume to find out the underlying ultrastructural phenotype. This shows NPC clusters exiting the nuclear envelope in proximity of ER double membranes that we hypothesize being phagophore membranes (due to the presence of Atg8 signal). If such hypothesis would be correct, we should be able to visualize autophagosomes containing nuclear pores in the cytoplasm and in the vacuole. We perform correlative light and electron microscopy using a tagged-Nup and an Atg15 knock-out strain (which does not allow the degradation of lipids in the vacuole). Unexpectedly we observe such autophagosomes containing double membrane vesicles owning NPCs both in the cytoplasm and in the vacuole (upon loss of one autophagic membrane due to the fusion with the vacuolar membrane). NPCs strikingly keep the same diameter and membrane curvature travelling form the nucleus to the vacuole, probably being still intact (7, 10) (Figure 3).

S. pombe NPC architecture in the cell and upon energy depletion

One prominent rearrangement we noticed in the structure of the NPC in the cell was its dilated configuration in comparison to previously published structures upon detergent purification (6) and upon nuclear envelope extraction (11) and we wanted to find perturbations that would trigger such changes in NPC diameter in the cellular context. With Dr. Christian Zimmerli we shifted to S. pombe as model organism because it was allowing us to have a higher throughput of tomograms in comparison to *S. cerevisiae*, Hela cells and *C. termophilum* (12). The structure of this NPC is dilated and owns a cytoplasmic ring where the Y-complex tail is missing, contradicting the dogma of a 3-ring scaffold assembly for the NPC. In collaboration with Sara Goetz and Ievgeniia Zagoriy from Julia Mahamid's group (EMBL) we looked at *S. pombe* cells upon energy depletion (the mitochondrial respiratory chain complex is inhibited by antimycin-A and 2-deoxy-glucose in the medium does not allow glucose hydrolysis) (13). ATP could not be produced by the cells simulating what happens when you extract the nuclear pore from its cellular context. In fact, the structure of the NPC shifted to this new medium showed a movement of the NPC scaffold towards a constricted configuration that we could model in collaboration with Kosinski's group (EMBL) (12) (Figure 4). This constriction of the NPC comes with a reduced nucleocytoplasmic transport as expected due to the lack of ATP, but also with a slower nucleocytoplasmic diffusion of small molecules like GFP that we demonstrate using Fluorescent Recovery After Photobleaching (FRAP). GFP diffusion rates into the nucleus decrease significantly upon energy depletion with a minimum after 1h of depletion, the time at which we solve the NPC structure (12).

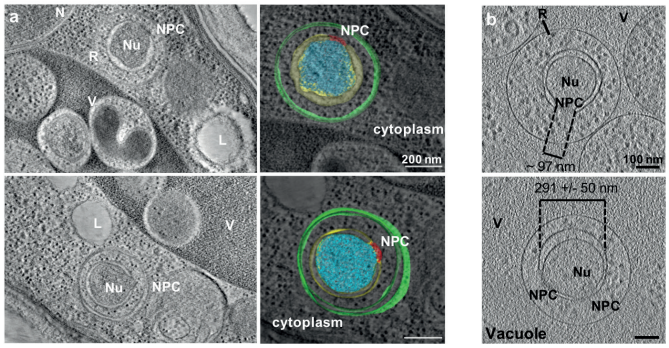

Figure 3: NPCs exit the nuclear envelope. a) Tomographic slice from plastic sections of 24h S. cerevisiae Atg15 knock-out strain starved of nitrogen for 24h. It shows a double membrane vesicle engulfing an NPC-containing nuclear vesicle. On the right, segmentation with NPC in red, nuclear content in blue, nuclear membrane in yellow and cytoplasmic double membrane in green. b) Cryo tomographic slice of the same strain in a) showing the presence of a normal-looking NPC engulfed in a vesicle in the vacuole. N is nucleus, V is vacuole, L is lipid droplet, R is ribosome, Nu is nuclear content, NPC is nuclear pore. Figure adapted from reference 7.

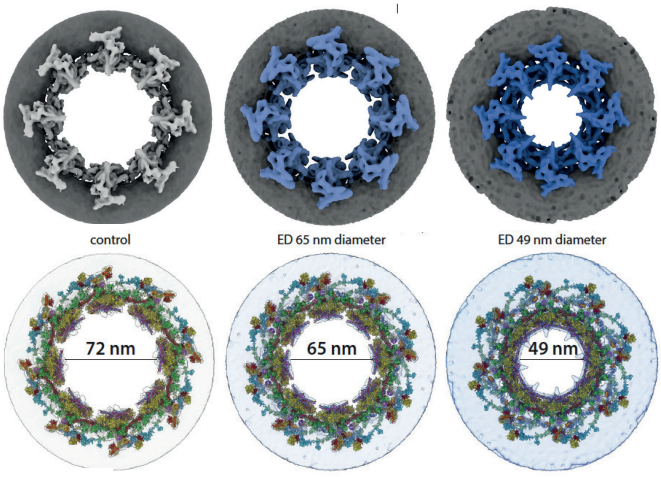

Figure 4: NPC constricts upon energy depletion. Subtomogram average (top) and corresponding integrative model (bottom) of S. pombe NPC in the cellular context upon energy depletion shows the conformational changes of the NPC scaffold due to the change of the energy status of the organism during control, intermediate and fully constricted NPC. The CR and IR move as individual entities and contribute more than the NR to the central channel volume reduction. Figure adapted from reference 13.

Summary

In summary using a combination of light, electron microscopy and molecular modelling methods we could solve high-resolution snapshots of the NPC in its cellular context, giving insights into its assembly and turnover pathways and we could show how different perturbations which simulate physiological cues can affect nuclear pore diameter and the architecture of the three scaffold rings. In particular we show a dilated nuclear pore that can be turnover by the autophagy machinery in a novel pathway where pieces of the nucleus containing NPCs are engulfed by double membrane autophagosomes (7, 10). In another case, we show how the change of the cell energy status in energy depleted conditions brings to NPC constriction (12). Our hypothesis is that such constriction increases the disordered barrier that molecules needs to pass in order to enter or exit the nucleus due to a reduction of around half of the size of the central channel NPC's volume (12). We are at the moment testing other physiological conditions that would lead to NPC dilation and constriction and affect molecule's transit through the NPC because such dynamics is fundamental for the passage of big cargos like HIV into the nucleus (we were able to show this in 14), and we know its importance for the passage of inner nuclear membrane proteins, for the assembly of the NPC, for cell differentiation, migration and nuclear mechanics.

Acknowledgements

I would like to thank my mentor Martin Beck for his continuous support, inspiration and freedom of research. I would like to thank Yannick Schwab, Paolo Ronchi, Wim Hagen, Felix Weis for the great help and the excellence of the electron microscopy at EMBL. I would like also to thank the members of Beck and Mahamid groups for the high level of intellectual exchange, the collaborative spirit and a lot of fun in diverse occasions. In addition I would like to thank Werner Kühlbrandt, Janet Vonck, Karen Davies, Thomas Meier, Deryck Mills and the extraordinary colleagues of the Max Planck Institute of Biophysics who marked my PhD experience. Finally I would like to thank Pierluigi Luisi and Pasquale Stano for training me with scientific and human values during my first year of academic research in Rome (Roma Tre University).

References

1) M. Beck, E. Hurt, The nuclear pore complex: understanding its function through structural insight. *Nat. Rev. Mol. Cell Biol.* 18, 73–89 (2017).
2) D. H. Lin, A. Hoelz, The Structure of the Nuclear Pore Complex (An Update). *Annu. Rev. Biochem.* 88, 725–783 (2019).
3) J. Mahamid, S. Pfeffer, M. Schaffer, E. Villa, R. Danev et al. Visualizing the molecular sociology at the HeLa cell nuclear periphery. *Science.* 351, 969–972 (2016).
4) M. Beck, V. Lŭ., F. Forster, W. Baumeister, O. Medalia et al. Snapshots of nuclear pore complexes in action captured by cryo-electron tomography. *Nature.* 449, 611–615 (2007).
5) J. Kosinski*, S. Mosalaganti*, A. Von Appen*, R. Teimer, A. L. Diguilio et al. Molecular architecture of the inner ring scaffold of the human nuclear pore complex. *Science.* 352, 363–568 (2016).
6) S. J. Kim*, J. Fernandez-Martinez*, I. Nudelman*, Y. Shi*, W. Zhang* et al. Integrative structure and functional anatomy of a nuclear pore complex. *Nature.* 555, 475–482 (2018).
7) M. Allegretti*, C. E. Zimmerli*, V. Rantos, F. Wilfling, P. Ronchi, et al. In-cell architecture of the nuclear pore and snapshots of its turnover. *Nature.* 586, 796–800 (2020).
8) SR. Wente, G. Blobel, A temperature-sensitive NUP116 null mutant forms a nuclear envelope seal over the yeast nuclear pore complex thereby blocking nucleocytoplasmic traffic. *J Cell Biol.* 123, 275-84 (1993).
9) E. Laudermilch, P.L. Tsai, M. Graham, E. Turner, C. Zhao et al. Dissecting Torsin/cofactor function at the nuclear envelope: a genetic study. *Mol. Biol. Cell* 27, 3964–3971 (2016).
10) C. W. Lee*, F. Wilfling*, P. Ronchi, M. Allegretti, S. Mosalaganti et al. Selective autophagy degrades nuclear pore complexes. *Nat. Cell. Biol.* 22, 159–166 (2020).
11) A. von Appen*, J. Kosinski*, L. Sparks*, A. Ori, A. L. DiGuilio et al. In situ structural analysis of the human nuclear pore complex. *Nature.* 526, 140–143 (2015).
12) C. E. Zimmerli*, M. Allegretti*, V. Rantos, S. K. Goetz, A. Obarska-Kosinska et al. Nuclear pores dilate and constrict in cellulo, Science doi: 10.1126/science.abd9776 (2021).
13) M. C. Munder, D. Midtvedt, T. Franzmann, E. Nüske, O. Otto et al. A pH-driven transition of the cytoplasm from a fluid- to a solid like state promotes entry into dormancy. *Elife.* 5:e09347 (2016).

14) V. Zila, E. Margiotta, B. Turoňová, T. G. Müller, C. E. Zimmerli et al. Cone-shaped HIV-1 capsids are transported through intact nuclear pores. *Cell.* 184, 1032-1046 (2021).
*shared authorship

Curriculum Vitae
Matteo Allegretti

Twitter: @Matteoffm
Web https://www2.mrc-lmb.cam.ac.uk/group-leaders/a-to-g/matteo-allegretti

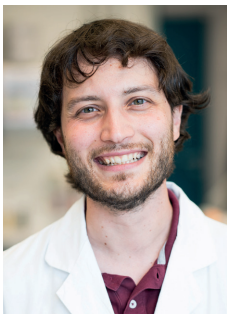

Matteo Allegretti
(Andreas Henn credit)

Matteo Allegretti studied biological sciences at the University of Roma Tre where he obtained his Master in biochemistry of macromolecules under the supervision of prof. Dr. Pierluigi Luisi with a thesis on lipid vesicles as cellular models in an origin-of-life scenario. Due to his passion for membrane systems, receptive borders between an internal and an external environment, he moved to the Max Planck Institute of Biophysics (Frankfurt am Main) as PhD student (2011) to investigate the structure/function of membrane proteins using cryogenic electron microscopy, in particular of mitochondrial ATP-synthases in the group of prof. Dr. Werner Kühlbrandt. During this period, he was funded by the IMPRS (International Max Planck Research School and Marie Curie Initial Training Network). As postdoc (2016), he decided to join Dr. Martin Beck group at EMBL to investigate the architecture of membrane proteins directly in their cellular context and upon environmental stresses, without the need of purification methods. During this period, he was funded by an EMBO and a Marie Curie individual fellowship. His focus has been since then on the investigation of nuclear pore complex and nuclear envelope remodeling, a hallmark of all eukaryotic cells. In 2022 he will move to the Laboratory of Molecular Biology (LMB-MRC) in Cambridge to start his own group on the macromolecular basis of compartment remodeling, where he will continue developing and using different imaging technologies to describe cellular mechanisms in four dimensions at different scales and resolutions. In LMB Matteo wants to continue to search the molecular principles which disclose the beauty of cellular organization trying to bridge structural, cell and developmental biology.

Quelle: Springer Spektrum Verlag

Über dieses Buch

Helmut Plattner nimmt Sie mit auf eine Zeitreise, die die Entwicklung der Zellbio-logie von der Erfindung des Mikroskops bis in unsere Zeit mit ihrem rasanten Fortschritt und dem Nobelpreis Physiologie/Medizin 2019 nachzeichnet. Neben seiner langjährigen Lehrerfahrung schöpft er v. a. daraus, dass er oft als (Zaun-)Gast oder sogar Akteur Teil dieser Entwicklung war. Modellorganismen von unterschiedlichem evolutionärem Niveau waren wichtige Hinweisgeber für Problemlösungen, besonders auch unter Einbeziehung neuer molekularbiologischer Methoden. Der Text ist verständlich geschrieben, zieht anschauliche Vergleiche und bietet Ihnen Anknüpfungspunkte durch bekannte Krankheiten (z. B. die Thematik Malaria und Sichel-zellanämie) und prominente Namen. Zahlreiche anschauliche Abbildungen runden den Text ab.

Der Autor

Helmut Plattner hat die Entwicklung der Zellbiologie und ihre Methodenentfaltung von der Pike auf aktiv miterlebt. Er leitete den Lehrstuhl für Zellbiologie an der Universität Konstanz von 1979 bis 2006 und setzte seine Forschungsarbeiten mit zahlreichen Kooperationen bis 2016 fort.

BINDER Innovation Prize

The RNA regulatory code of cell fate decisions

Leo Kurian

Summary

A central question in cell and developmental biology is how the genetic information is differentially interpreted to enable cell-fate transitions and the conferring of cellular identity. In this regard, the last decades have mainly focused on morphogen-mediated signal transduction, epigenetic, and transcriptional mechanisms. However, RNA is the universal language primarily used for the first layer of communication from the genome. Apart from acting as an accurate template for the synthesis of proteins, RNA carries a compendium of embedded codes that instruct and control the forward communication of genetic information, ranging from how the message from the genome is processed, spliced; to how, when, and where mRNAs are translated, the rules of which remains to be fully understood. Besides, <95% of the RNA encoded by the genome do not template for protein synthesis, but function as RNA molecules (non-coding RNAs), whose molecular function, physiological role, and mechanisms remain unclear. Coding and non-coding transcripts are further instructed by ~2500 RNA binding proteins (RBPs), thus constructing intricate RNA-centric regulatory networks. These RNA regulatory networks or RNA regulons present a highly complex yet poorly understood RNA-centric regulatory matrix, and RNA regulons are proposed to play a deterministic role in the foundation of cellular fate and function during embryogenesis, especially in vertebrates. In this regard, fate specific lncRNAs and regulators of translation remains particularly enigmatic. We discovered that divergently transcribed lncRNAs, originating from loci encoding developmental regulators are central to embryonic cell fate decisions. Mechanistic studies on one the newly identified divergent lncRNAs, *YYLNCT*, revealed how de novo DNA methylation is regulated by local inhibition of DNMT3B by lncRNAs. To systematically investigate the role of translational control mechanisms in mediating cell fate decisions, we first developed a new method to comprehensively survey auxiliary factors sequestering on active ribosomes (Active ribosome capture mass spectrometry, ARC-MS). By applying ARC-MS in human pluripotent stem cells and mesoderm progenitors, we discovered fate-specific interactors of active translational complexes. RNA binding proteins were the most abundant class of proteins sequestering on active ribosomes. Notably, we discovered proteins involved in transcription, mRNA splicing, nucleolar control, signal transduction, and energy metabolism to associate with active ribosomes. Based on our findings, we propose that ribosomes act as unifying hubs for cellular decision-making by directly communicating with vital macromolecular complexes controlling fundamental cellular processes during embryonic cell-fate decisions. Taken together, our long-term goal is to gain a systems-level understanding of the RNA-codes that encrypt cellular identity and homeostasis in humans (Figure 1).

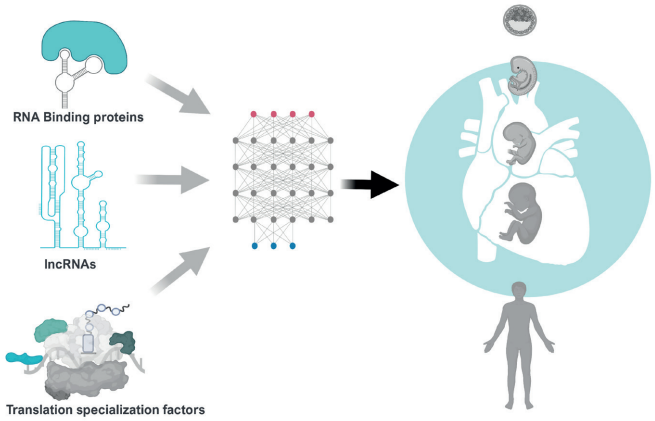

Figure 1: The RNA regulatory code of cell fate decisions: Illustration of the overarching hypothesis: 'Cooperative regulation of gene expression machines by RNA regulons control embryonic cell fate decision (using cardiac development and homeostasis as models)'.

YYLNCRNAs, a new class of divergent lncRNAs

The acquisition of cellular identities during embryonic development is a well-concerted, precisely timed, and robustly executed process[1]. This relies on the timely and coordinated expression of cohorts of genes, which determine a particular cellular state, defining its transcript repertoire. While the embryo progresses through development, new transcriptional programs are established with precision to enable successful differentiation into a given lineage. Although the identity and function of many of these lineage-defining core transcriptional networks are characterized, the mechanisms that regulate and coordinate these processes that allow embryonic developmental transitions remain poorly understood, especially in humans[2-4].

Long non-coding RNAs (lncRNAs) that are transcribed at bidirectional promoters (divergent lncRNAs) are emerging as critical regulatory components of local gene expression, especially in murine models for embryonic development[5,6]. To determine the prevalence of cell-type/ developmental stage-specific divergent

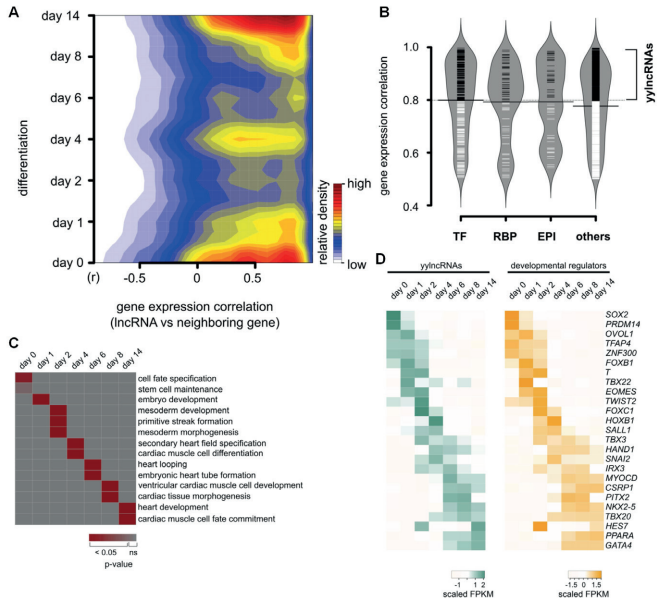

Figure 2: YYLNCRNAs, a new class of divergent lncRNAs: (A) Divergent lncRNAs are a prevalent feature during cardiogenesis in vivo in mice. Correlation-based density distribution of the gene expression dynamics of the divergent lncRNAs with respect to their neighboring genes. (B) Gene expression correlation distributions of the differentially expressed divergent lncRNAs with respect to the neighboring genes for the indicated gene categories. TF: Transcription factors; RBP: RNA binding proteins; EPI: Epigenetic regulators. (C) Prominent GOs, curated based on significance for the accompanying protein-coding neighbors of yylncRNAs (p-value < 0.05). (D) The expression dynamics of a representative set of currently unannotated yylncRNAs that accompany key developmental genes.

lncRNAs during early cell-fate decisions of human embryonic stem cells (hESCs), we performed an in-depth sequencing of total RNA (ribosome-depleted) from seven defined stages of cardiac commitment[4,7-10]. Using our RNA-seq compilation, we identified 8329 bidirectionally-transcribed loci, encoding lncRNA-protein-coding gene pairs, of which 6425 remain currently unannotated (for lncRNAs: minimum FPKM value 0.5, minimum length 1kb, distance to the neighboring protein-coding genes TSS ≤500bp) (Figure 2A). Approximately 73% of these divergent lncRNAs were polyadenylated, as revealed by transcriptome sequencing after polyA enrichment. To test the in vivo relevance and potential evolutionary conservation of this observation, we performed whole transcriptome sequencing of micro-dissected cardiogenic regions from E8 (heart tube), E8.5 (looping heart tube), E9.5 (looped heart tube), and E14 (chambered embryonic heart) mouse embryos. Divergent transcription was prevalent during cardiac commitment in vivo, with significant syntenic conservation at 4403 loci between corresponding time points along hESC-differentiation8,11.

Divergent lncRNAs often show expression patterns similar to their corresponding neighboring genes, indicative of regulation in cis12. The majority of identified divergent lncRNAs showed similar expression dynamics as their neighboring protein-coding gene (with 6887 having r > 0). Importantly, this phenomenon was conserved during cardiogenesis in vivo. Differential gene expression analysis revealed that 3012 divergent lncRNAs showed cell-type specificity in their expression dynamics (fold enrichment > 2, p-value < 0.001). The protein-coding genes paired to differentially expressed lncRNAs were involved in regulating developmental cell-fate transitions leading to cardiogenesis, significantly more than those accompanying non-differentially expressed lncRNAs. Interestingly, we discovered that those protein-coding genes that accompany divergent lncRNAs, which show a near-identical expression pattern (r ≥ 0.8), were key regulators of each of the cell-fate transitions essential for acquiring the cardiac identity (Figure 2C). We classified this class of divergent lncRNAs as yylncRNAs ("yin yang": signifying their mirrored genomic arrangement and near-identical expression pattern). Transcription factors (n=176) were the largest gene category physically paired to yylncRNAs (Figure 2B). Importantly, we identified 781 YYLNCRNAs expressed from genomic loci encoding key regulators of cardiac cell fate decisions, revealing a new class of developmentally regulated genes. Notably, we discovered YYLNCRNAs expressed from loci encoding central regulators of cardiac cell fate decisions, including *TBXT (T), EOMES, TWIST2, FOXC1, SNAI2, HAND1, HAND2, GATA6, NKX2.5, GATA4, TBX20* (Figure 2D).

YYLNCT is essential for mesoderm cell fate decision

While we discovered prevalent, near identically transcribed divergent lncRNAs emerging from loci encoding cell fate reg-

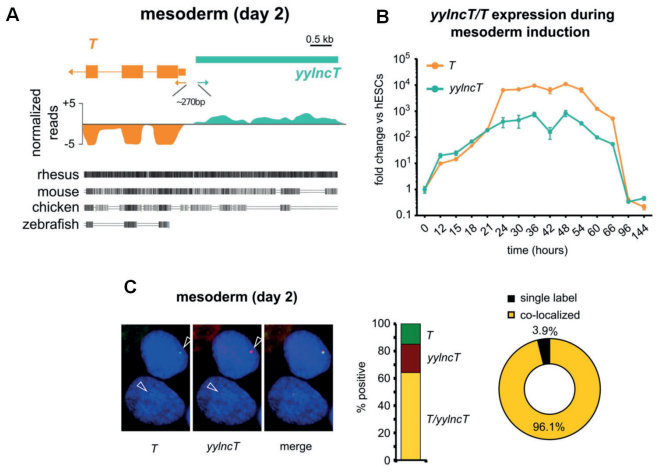

Figure 3: YYLNCT is encoded from and associated with the T locus during mesoderm commitment: (A) Schematic representation of the T locus showing strand-specific expression of T and YYLNCT and their sequence conservation (chr6:166157656-166171377; hg38). (B) Co-expression of YYLNCT and T during mesoderm induction. (C) Two-color single molecule RNA-FISH of YYLNCT (red) and T (green) in mesodermal cells derived from hESCs and their quantification (n=67). Micrographs depicted here as a composite image of blue and red/green channel as well as all channels.

ulators, their molecular and developmental function remains unknown. Next, based on their expression specificity and the developmental relevance of the encoding genomic loci, we hypothesized that yylncRNAs can assume regulatory roles in developmental cell-fate transitions. To test this hypothesis, we chose a currently unannotated yylncRNA transcribed from the BRACHYURY (T) locus, which we termed as *'YYLNCT'* (Figure 3A). T is a conserved master regulator of mesoderm development. *YYLNCT* is specifically expressed in the mesoderm stage of cardiac commitment along with T. It is transcribed ~270bp upstream to the transcriptional start site of T, giving rise to a polyadenylated, single-exonic transcript of 3253 nucleotides. YYLNCT is an abundant transcript displaying a near-identical expression pattern to T during mesoderm commitment of hESCs (Figure 3B). YYLNCT localized to a single spot in the nucleus in mesoderm-committed hESCs, revealed by single-molecule RNA-FISH (Figure 3C). Importantly, *YYLNCT* localizes to actively transcribing T-locus, as revealed by co-localization of *YYLNT* and a set of probes marking RNA copied from the first intron of T. Thus *YYLNCT* transcript marks the active T locus during mesoderm commitment of hESCs.

Next, we investigated the functional role of *YYLNCT* in the context of mesoderm differentiation of hESCs. We hypothesized that the genomic region encoding *YYLNCT* could assume a functional role (i) by serving as a DNA regulatory region, (ii) by virtue of its transcription alone, or (iii) by an RNA-mediated function. First, we employed a polyA knock-in strategy to disrupt *YYLNCT* transcription at 1036bps downstream to its transcriptional start site (TSS) (Figure 4A). This strategy allows productive transcription to persist up to the site of insertion of the polyA signal, leading to a 3' end truncation of 2217 nucleotides. Upon induction to the mesoderm, the polyA-insertion clones failed to activate T, despite expressing the truncated *YYLNCT* (Figure 4B). This suggests that the production of a full-length *YYLNCT* is required for the activation of T and that *YYLNCT* locus might be not be functioning by virtue of its transcription alone.

Next, to test whether *YYLNCT* exerts this activating function as a transcript, we employed three independent antisense oligos, including two different chemistries (ASOs and 2'-deoxy-2'-fluoroarabinonucleic acid, FANA-ASOs) to specifically deplete the *YYLNCT* transcript without changing its genomic sequence. ASO-mediated depletion of the *YYLNCT* transcript led to a significant decrease in T levels, as well as to other early mesoderm markers, suggesting that *YYLNCT* is an upstream mediator of the mesoderm fate of hESCs. Transcriptomic profiling of hESCs induced to mesoderm upon depletion of *YYLNCT* showed strong and reproducible defects in the activation of early mesodermal genes, indicating an inability to differentiate to mesoderm (Figure 4C). Importantly, *YYLNCT* depletion led to a significant decrease in the expression of validated targets of T, which are key drivers of mesoderm fate (Figure 4C, heatmap). This led to dramatically lower levels of T protein upon mesoderm induction. Mesoderm induction upon loss of *YYLNCT* resulted in apoptosis, while it did not affect the ability of hESCs to undergo endoderm and ectoderm commitment (Figure 4D). Thus we revealed a so far unknown regulator of mesoderm cell-fate decision.

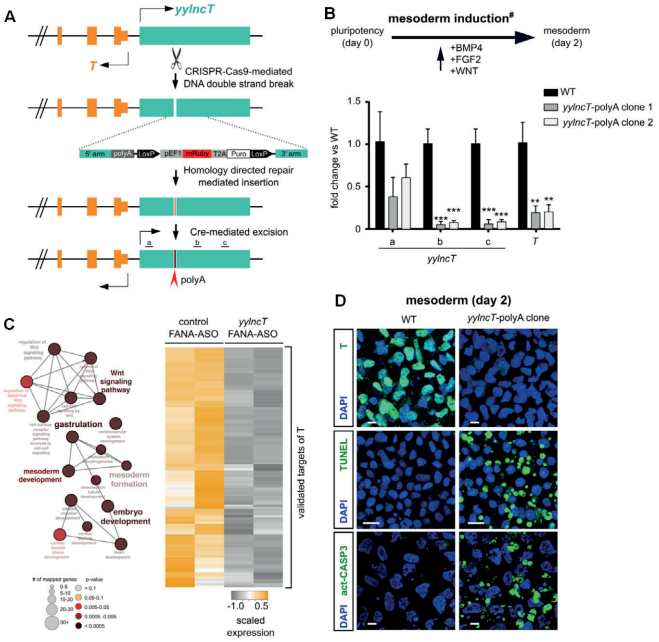

Figure 4: YYLNCT is essential for mesoderm cell fate decision: (A) Outline of the strategy employed to impede YYLNCT transcription by insertion of a polyA sequence. (B) Relative expression of YYLNCT and T upon mesoderm differentiation of the indicated clones (a, b, and c = RT-qPCR primer pairs). (C) GO enrichment analysis of differentially expressed transcripts upon YYLNCT knockdown. Heatmap depicting downregulation of validated T targets upon YYLNCT knockdown. (D) Downregulation of T and the induction of apoptosis in the indicated cell lines. Micrographs depicted here as a composite image of blue and green channel. Data are represented as mean ± SEM. Scale bar = 10µm.

YYLNCT prevent aberrant DNA methylation at BRACHYURY locus by local inhibition of DNMT3B

In an effort to gain further molecular and mechanistic insights on *YYLNCT*, we performed "chromatin oligo affinity precipitation" (CHOP) followed by mass spectrometry (MS)12,13 in the indicated conditions to identify its protein interacting partners using biotinylated, nested oligos (Figure 5A, 5B). We identified 110 proteins specifically binding *YYLNCT* in mesoderm-committed hESCs. We reasoned that, since *YYLNCT* is a nuclear lncRNA localizing to the T locus, a relevant interacting partner might have both RNA and DNA-binding ability. 21 *YYLNCT*-interacting proteins are annotated to have these characteristics and the majority of them showed a mesoderm-specific expression similar to *YYLNCT/T* (Figure 5C). We chose the de novo DNA methyltransferase DNMT3B, for further investigation, since during early lineage commitment of pluripotent stem cells, de novo DNA methylation builds an epigenetic barrier, restricting the differentiation potential and preventing the regression back

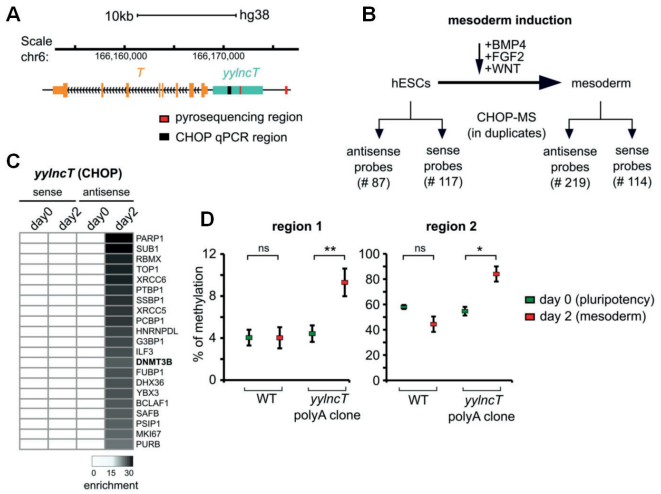

Figure 5 YYLNCT prevent aberrant DNA methylation at BRACHYURY locus by local inhibition of DNMT3B. (A) Genome browser depiction of the T and YYLNCT genomic loci (chr6:166157656-166173512; hg38). (B) CHOP-MS experimental strategy to identify specific interactors of YYLNCT in upon mesoderm commitment of hESCs. (C) Heatmap representing the specific enrichment of YYLNCT bound proteins in mesoderm. (C) Percentage increase in methylation in YYLNCT-polyA clone over WT at the mesodermal stage. Data are represented as mean ± SEM.

to pluripotency14. Besides DNMT3B none of the *YYLNCT*-binding proteins have a known role in the lineage commitment of hESCs. Additionally, *YYLNCT* did not show any interaction with proteins reported to regulate functional lncRNAs, including members of the mediator complex and PRC complex. The interaction of *YYLNCT* to DNMT3B was orthogonally confirmed by RNA immunoprecipitation (RIP) for DNMT3B followed by RT-qPCR. Since genome-wide de novo methylation, mainly mediated by DNMT3B, is one of the first epigenetic barriers created upon lineage commitment of hESCs, we hypothesized that its methylation activity at the T locus might be locally regulated by virtue of its association with *YYLNCT*. Notably, the majority of early developmental loci seldom undergo de novo DNA methylation during lineage commitment when hESCs leave the state of pluripotency. If our hypothesis is correct, we should detect an increase in methylation levels in the differentially-methylated region of *YYLNCT* (regions 1 and 2 picked based on available bisulfite sequencing data, in our YYLNCT-polyA clones upon mesoderm induction. Targeted DNA methylation analysis in these regions using pyrosequencing (at the stage of pluripotency and upon induction of mesoderm) indicated that in the absence of a functional *YYLNCT* transcript, both regions show significantly elevated methylation compared to the wild-type scenario (Figure 5D). This supports our hypothesis, whereby local inhibition of DNMT3B by *YYLNCT* keeps the *T/YYLNCT* locus hypomethylated during mesoderm commitment of hESCs. While genome-wide de novo methylation is the norm during early developmental fate transitions, the mechanisms by which the key developmental loci are locally protected from de novo methylation remain unclear. Based on our data, we propose that a yylncRNA-mediated transient and local inhibition of de novo DNA methylation is one mechanism by which developmental loci retain their hypomethylated status.

Outlook: Taken together, here we defined a new class of divergent lncRNAs, yylncRNAs (781 yylncRNAs of which 491 were hitherto unannotated; genomic coordinates and expression dynamics) along cardiac differentiation alone)6. Importantly, by focusing on *YYLNCT*, an unannotated lncRNA paired with the master mesoderm regulator T, we showed that it acts as an essential activator of the T locus by locally modulating de novo DNA methylation by DNMT3B during mesoderm differentiation. Finally, considering that loci expressing multiple yylncRNAs show similar trends in DNA methylation dynamics as T/YYLNCT loci, it is plausible that these yylncRNAs safeguard developmental loci from aberrant de novo methylation. However, considering the versatility of RNA-mediated gene regulation, as well as recent reports in mice on relatively similar regulatory lncRNAs, the mechanisms and extent of regulatory properties need to be tested on an individual basis since they might vary in a case/context-dependent manner. In conclusion, yylncRNAs add a layer of complexity to the gene regulatory networks that mediate cell-fate transitions during the differentiation of pluripotent stem cells.

Translational specialization of cell fate decisions and cellular identity

The success of developmental cell-fate decisions relies on the timely, specific, accurate, and efficient rewiring of the gene regulatory networks to support rapid cellular identity changes[15,16]. In this regard, the last decades have mainly focused on morphogen-mediated signal transduction, epigenetic, and transcriptional mechanisms[17]. However, translational control (regulation mRNA translation) is the primary determinant of protein abundance in mammals[18,19]. While poorly understood, translational control is proposed to be vital during embryogenesis[20,21]. Analysis of the transcripts associated with various ribosomal complexes derived from mouse ES cells (mESC) in comparison to differentiated embryoid bodies revealed that mESCs are uncharacteristically dependent on monosomes for protein synthesis. Elegant in vivo studies using deep sequencing of ribosome-protected RNA fragments (ribo-seq) suggested that mesoderm lineage is particularly dependent on translational control at the exit of pluripotency. Notably, apart from general translational control, key signaling cascades that drive mesoderm development, including Wnt, Shh, Hippo, PI3k, and Mapk, are proposed to be directly regulated by their selective translation in mice[22]. Translational control has been suggested to be of paramount importance during the maternal-zygotic transition and in the regulation of Hox mRNAs[23]. Reinforcing the proposed seminal role for translational control and its role in tissue-specific gene

regulation, mutations in components of translational machinery lead to markedly distinct phenotypes across phyla, indicating their specialized function. Conceptually, as postulated by elegant studies using murine in vitro and in vivo models, apart from accurate, rapid, and 'on demand' control of gene regulation, translational control allows much-needed energy conservation during early embryogenesis when energy is limited. Despite these evidence, how embryonic translation is selectively regulated, its functional role, its mediators and mechanisms, and its regulatory principles remain a fundamental gap in our current understanding of the molecular control of embryonic development.

Active Ribosome Capture-Mass Spectrometry (ARC-MS) to identify regulators of selective mRNA translation

We hypothesized that the developmental competence for cell-fate transitions is translationally controlled and dependent on the fate-specific modular composition of ribosomal complexes, harboring translation specialization factors (TSFs). TSFs- program the selective and privileged translation of developmental genes in defined time windows to enable cell-fate acquisition and maintenance of cellular identity. Thus TSFs preferentially sequester on actively translating ribosomes (active ribosomes), either directly or through their interaction with target mRNAs in a cell fate-specific manner to control ribosomal output. Identification of cell fate-specific TSFs is technically challenging due to the following reasons.

Current methods used for identifying TSFs either (i) require the generation of engineered ribosomal proteins, (ii) suffer from contamination of unrelated protein complexes, or (iii) unable to distinguish de novo synthesized proteins from TSFs. In addition, during the early stages of embryogenesis, a significant fraction of ribosomes are inert and ribosomal proteins are generated in excess. We reasoned that a thorough proteomic characterization of active ribosomes in a cell type-specific manner combined with simultaneous separation of ribosomal components and associated proteins from de novo synthesized proteins will be an ideal strategy to identify TSFs. For this purpose, we developed Active Ribosome-Mass spectrometry (ARC-MS) to identity TSFs. ARC-MS involves the labeling of de novo synthesized proteins using brief pulse with a cell-permeable, 'clickable' methionine analog, a proprietary derivative of non-canonical amino acid L-azidohomoalanine, AHA, followed by stably anchoring labeled nascent peptides using a translational inhibitor. Next, upon lysis under RNAse-free and ribosome-protected conditions, active ribosomal complexes are isolated by click reaction. After high salt washes to exclude nonspecific interactions, an 8M urea wash in denaturing conditions allows the faithful separation of ribosomal complexes, translation factors, and TSFs from de novo synthesized nascent proteins and quantitatively detected using liquid chromatography coupled mass spectrometry. TSFs are identified by filtering out known ribosomal proteins, translation factors and de novo synthesized proteins. By virtue of the short AHA labeling, ARC-MS captures ribosomal complexes at the early stages of translation, arguably the rate-limiting and most regulated steps of protein synthesis, further increasing the probability of identifying TSFs.

As a proof of principle, we performed ARC-MS in pluripotent stem cells and hPSC-derived mesodermal cells. Ribosomal proteins, translational initiation, and elongation factors occupied the majority of top enriched proteins, demonstrating successful isolation of active ribosomes (Figure 6A). Excluding known ribosomal proteins and translation factors, we identified 768 proteins as candidate TSFs. Proteins involved in crucial cellular processes, including transcriptional regulation, mRNA splicing, RNA export, mRNA processing, mRNA stability, energy metabolism, and developmental signaling were found to sequester on actively translating ribosomes (Figure 6B). This includes proteins belonging to complexes previously suggested to communicate with ribosomal complexes and regulate translation, including PKM, DDX39B, HNRNPU, components of proteasome, CDC42,

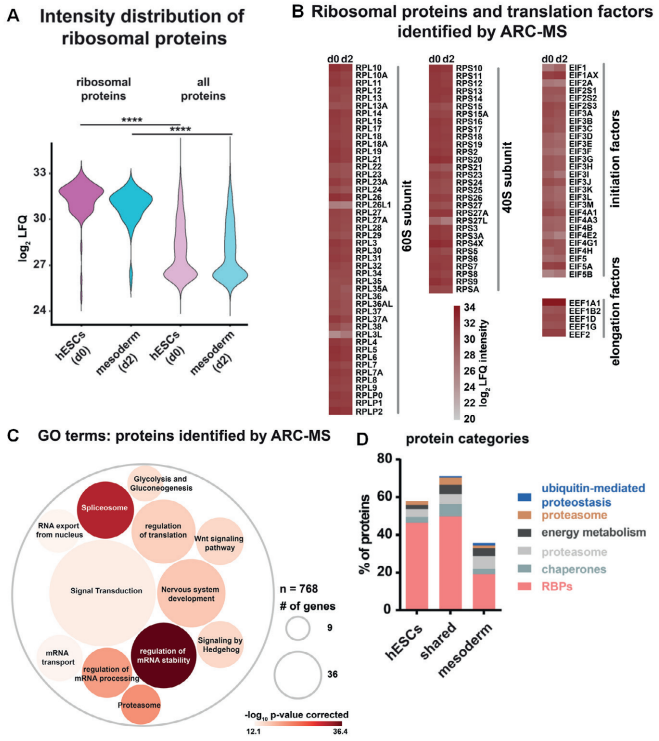

Figure 6: Active Ribosome Capture-Mass Spectrometry (ARC-MS) to identify regulators of selective mRNA translation: (A) Ribosomal proteins are the most enriched proteins in ARC-MS, revealing the validity of our method. (B) Distribution of known ribosomal protein, translation initiation and elongation factors with the ARC-MS data. (C) Functional annotation of proteins sequestering on active ribosomes in pluripotency and mesoderm illustrating unprecedented cross talk between myriad cellular processes and ribosomes. (D) Main protein categories represented in the unique and shared ribosome-associated proteomes of hESCs Vs mesoderm.

and G3BP2. The majority of the identified proteins were RNA binding proteins, including bona fide regulators of selective translation controlling cell fate decisions, including LIN28, PABPC1, NONO, FXR1, and IGF2BP1 (Figure 6C). Of the 768 candidate-TSFs identified, 96 and 73 showed preferential enrichment on ribosomes in hPSCs and mesodermal cells, respectively, thus providing proof of principle to our initial hypothesis. Taken together, we provide a fertile ground for future research to carefully investigate the role of these cell fate-specific factors to regulate (i) translation, (ii) morphogenesis, and iii) the mechanisms by which they operate[24].

Outlook

Owing to the identification of proteins involved in multiple cellular processes to be sequestering on active ribosomes, we postulate that ribosomes act as a real-time control hub for cellular decision making, constantly in communication with vital macromolecular complexes controlling fundamental cellular processes and selectively regulating the abundance of functional proteins. This contributes to the maintenance of fidelity in gene expression by ensuring that proteins required for a specific process/ stimuli are synthesized only when needed in the right amount upon directly communicating with regulatory affector- pathways[25]. For example, direct communication with regulators of metabolism could allow the metabolic machinery to directly control translation, the most energy demanding cellular process, to keep a check on energy exhaustion and associated cellular stress response (Figure 7). This postulation is supported by evidence from bacteria[26], yeast[27] and mice[28] demonstrating the direct interaction between ribosomes with protein complexes controlling transcription, mRNA splicing, metabolism and protoestasis aligning with our findings, while functional implications of such interactions remains unclear. We envision this currently understudied layer of translational specialization to substantially impact our understanding of gene regulation in myriad avenues from embryogenesis to congenital and adult-onset disease. In support of this notion, many RBPs identified in our ARC-MS as candidate TSFs are associated with congenital and adult-onset neuronal and cardiac disorders. We are committed to carefully investigate the role of translational specialization to advance our currently rudimentary understanding of the translation control of human development as a prelude to developing new therapeutic innovations[24,29].

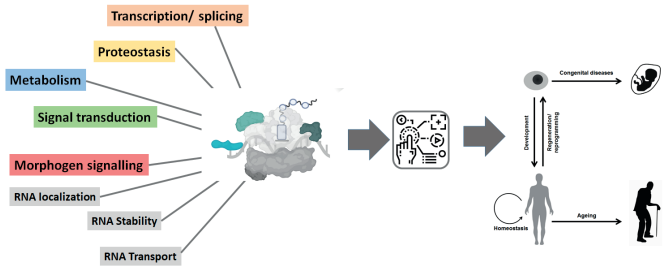

Figure 7: Translational specialization of cell fate decisions hypothesis: Ribosomes act as a unifying cooperativity hubs for cellular decisions by directly communicating with vital macromolecular complexes that control fundamental cellular processes and decide the timely de novo synthesis of regulatory factors.

Acknowledgement

I express my heartfelt gratitude to the present and past members of my lab, whose tireless efforts led to the findings presented here. I respect their bravery to join me in my new lab back in 2014, build a cohesive environment that allowed us to challenge our scientific outlook, try our very best to do innovative research, and contribute to fundamental understanding of the logic of gene regulation. I want to thank the efforts of Stefan Frank and Gaurav Ahuja, who spearheaded the first publications from the lab. Importantly, I salute the beyond-heroic efforts, dedication, consistent commitment by Deniz Bartsch, who established the work on translational control and helped the lab and me through the turbulent last years. I thank the effort by talented Wenjie Yao and Kaustubh Kalamkar, whose findings on mRNA splicing and ribosome biogenesis I could not include here. They inspire me every day, teach me lessons in science and life that enable me to try to lead the lab to the best of my abilities, and create an environment where science always takes prominence. Watching them blossom in science and in life has been the biggest joy in my career so far, and I feel immensely privileged to work with them. I thank Prof. Thomas Benzing, Dr. Debra Grosskopf, Prof. Jürgen Hescheler for constantly supporting us over the years. I am grateful to our host institutes CMMC, CECAD, and the Faculty of Medicine, the University of Cologne and hope that they will provide long term which would allow us to continue our efforts. I am indebted to patient advice and guidance by my mentors and advisors Prof. Jürgen Dohmen (University of Cologne), Prof. Juan Carlos Izpisua Belmonte (The SALK Institute for Biological Studies), Prof. Gene Yeo (University of California San Diego), Prof. Thomas Langer (MPI-AGE) and Prof. Alexandra Trifunovic. Our work will not be possible without our brilliant and ever-supportive collaborators. We thank our collaborators from the industry, especially Immagina Biotech (Italy) and U1 Bio (San Fransisco). Finally, the work in our lab will not be possible without the generous funding over the years by NRW Stem Cell Network Grant (No: 3681000801 and 2681101801), Else Kröner-Fresenius-Stiftung (Grant No:3640 0626 21), Deutsche Forschungsgemeinschaft (DFG), and Center for Molecular Medicine Cologne (CMMC, ZMMK Grant No: 3622801511), Köln Fortune and DZHK.

About the author

Curriculum Vitae

Leo Kurian studied the mechanisms controlling fidelity of translation and ribosomal frameshifting, earning his Ph.D. degree in 2009 at the Institute for Genetics, University of Cologne. For his postdoctoral work, he moved to the Salk Institute for Biological Studies, San Diego, California, followed by the University of California San Diego (UCSD) where he developed embryonic stem cell-based models recapitulating human early embryonic cell fate decisions and initiated his efforts on understanding the role of RNA regulons. In 2014 upon receiving the NRW Stem Cell Network Independence Grant, he returned to the University of Cologne, where he established his independent group at the Center for Molecular Medicine, Faculty of Medicine. He is the recipient of German Stem Cell Network (GSCN) Young Investigator Award in 2016.

References

1 Spemann, H. & Mangold, H. Induction of embryonic primordia by implantation of organizers from a different species. 1923. *The International journal of developmental biology* **45**, 13-38 (2001).

2 Gerrard, D. T. et al. An integrative transcriptomic atlas of organogenesis in human embryos. *eLife* **5**, doi:10.7554/eLife.15657 (2016).

3 Tsankov, A. M. et al. Transcription factor binding dynamics during human ES cell differentiation. *Nature* **518**, 344-349, doi:10.1038/nature14233 (2015).

4 Kurian, L. et al. Identification of novel long noncoding RNAs underlying vertebrate cardiovascular development. *Circulation* **131**, 1278-1290, doi:10.1161/CIRCULATIONAHA.114.013303 (2015).

5 Engreitz, J. M. et al. Local regulation of gene expression by lncRNA promoters, transcription and splicing. *Nature* **539**, 452-455, doi:10.1038/nature20149 (2016).

6 Ulitsky, I., Shkumatava, A., Jan, C. H., Sive, H. & Bartel, D. P. Conserved function of lincRNAs in vertebrate embryonic development despite rapid sequence evolution. *Cell* **147**, 1537-1550, doi:10.1016/j.cell.2011.11.055 (2011).

7 Cai, W. et al. Coordinate Nodal and BMP inhibition directs Baf60c-dependent cardiomyocyte commitment. *Genes & development* **27**, 2332-2344, doi:10.1101/gad.225144.113 (2013).

8 Kuo, C. C. et al. Detection of RNA-DNA binding sites in long noncoding RNAs. *Nucleic acids research* **47**, e32, doi:10.1093/nar/gkz037 (2019).

9 Kurian, L. et al. Conversion of human fibroblasts to angioblast-like progenitor cells. *Nature methods* **10**, 77-83, doi:10.1038/nmeth.2255 (2013).

10 Mondal, T. et al. Sense-Antisense lncRNA Pair Encoded by Locus 6p22.3 Determines Neuroblastoma Susceptibility via the USP36-CHD7-SOX9 Regulatory Axis. *Cancer cell* **33**, 417-434 e417, doi:10.1016/j.ccell.2018.01.020 (2018).

11 Frank, S. et al. yylncT Defines a Class of Divergently Transcribed lncRNAs and Safeguards the T-mediated Mesodermal Commitment of Human PSCs. *Cell stem cell* **24**, 318-327 e318, doi:10.1016/j.stem.2018.11.005 (2019).

12 Luo, S. et al. Divergent lncRNAs Regulate Gene Expression and Lineage Differentiation in Pluripotent Cells. *Cell stem cell* **18**, 637-652, doi:10.1016/j.stem.2016.01.024 (2016).

13 Mondal, T. et al. MEG3 long noncoding RNA regulates the TGF-beta pathway genes through formation of RNA-DNA triplex structures. *Nature communications* **6**, 7743, doi:10.1038/ncomms8743 (2015).

14 Lister, R. et al. Human DNA methylomes at base resolution show widespread epigenomic differences. *Nature* **462**, 315-322, doi:10.1038/nature08514 (2009).

15 Newport, J. & Kirschner, M. A major developmental transition in early Xenopus embryos: II. Control of the onset of transcription. *Cell* **30**, 687-696, doi:10.1016/0092-8674(82)90273-2 (1982).

16 Xiang, L. et al. A developmental landscape of 3D-cultured human pre-gastrulation embryos. *Nature* **577**, 537-542, doi:10.1038/s41586-019-1875-y (2020).

17 Loh, K. M. et al. Mapping the Pairwise Choices Leading from Pluripotency to Human Bone, Heart, and Other Mesoderm Cell Types. *Cell* **166**, 451-467, doi:10.1016/j.cell.2016.06.011 (2016).

18 Kristensen, A. R., Gsponer, J. & Foster, L. J. Protein synthesis rate is the predominant regulator of protein expression during differentiation. *Molecular systems biology* **9**, 689, doi:10.1038/msb.2013.47 (2013).

19 Schwanhausser, B. et al. Corrigendum: Global quantification of mammalian gene expression control. *Nature* **495**, 126-127, doi:10.1038/nature11848 (2013).

20 Ingolia, N. T., Lareau, L. F. & Weissman, J. S. Ribosome profiling of mouse embryonic stem cells reveals the complexity and dynamics of mammalian proteomes. *Cell* **147**, 789-802, doi:10.1016/j.cell.2011.10.002 (2011).

21 Genuth, N. R. & Barna, M. Heterogeneity and specialized functions of translation machinery: from genes to organisms. Nature reviews. *Genetics* **19**, 431-452, doi:10.1038/s41576-018-0008-z (2018).

22 Fujii, K., Shi, Z., Zhulyn, O., Denans, N. & Barna, M. Pervasive translational regulation of the cell signalling circuitry underlies mammalian development. *Nature communications* **8**, 14443, doi:10.1038/ncomms14443 (2017).

23 Shi, Z. & Barna, M. Translating the genome in time and space: specialized ribosomes, RNA regulons, and RNA-binding proteins. *Annual review of cell and developmental biology* **31**, 31-54, doi:10.1146/annurev-cellbio-100814-125346 (2015).

24 Bartsch, D. et al. Translational specialization in pluripotency by RBPMS poises future lineage-decisions. *bioRxiv*, 2021.2004.2012.439420, doi:10.1101/2021.04.12.439420 (2021).

25 Kurian, L., Palanimurugan, R., Godderz, D. & Dohmen, R. J. Polyamine sensing by nascent ornithine decarboxylase antizyme stimulates decoding of its mRNA. *Nature* **477**, 490-494, doi:10.1038/nature10393 (2011).

26 Butland, G. et al. Interaction network containing conserved and essential protein complexes in Escherichia coli. *Nature* **433**, 531-537, doi:10.1038/nature03239 (2005).

27 Vo, T. V. et al. A Proteome-wide Fission Yeast Interactome Reveals Network Evolution Principles from Yeasts to Human. *Cell* **164**, 310-323, doi:10.1016/j.cell.2015.11.037 (2016).

28 Simsek, D. et al. The Mammalian Ribo-interactome Reveals Ribosome Functional Diversity and Heterogeneity. *Cell* **169**, 1051-1065 e1018, doi:10.1016/j.cell.2017.05.022 (2017).

29 Ju Lee, H. et al. A post-transcriptional program coordinated by CSDE1 prevents intrinsic neural differentiation of human embryonic stem cells. *Nature communications* **8**, 1456, doi:10.1038/s41467-017-01744-5 (2017).

Werner Risau Prize

Oligodendrocyte precursor cell specification is regulated by bidirectional neural progenitor–endothelial cell cross-talk

Isidora Paredes Ugarte

Summary

Neurovascular communication assures proper central nervous system (CNS) development, sustains homeostasis and instructs repair. Yet, the molecular mechanisms that regulate such communication are still not fully characterized. While we are starting to understand how neural-derived signals are crucial regulators of CNS vascularization, it still remains largely unknown how the vasculature responds to these signals. This study highlights how a precise coordination between the vascular and nervous system is required for OPC specification. It describes a functional active bi-directional molecular cross-talk between neural progenitor cells (NPCs) and endothelial cells (ECs) of the growing vasculature required for for promoting oligodendrocyte precursor cell (OPC) specification in the developing CNS *in vivo*. This signaling axis involves neural-derived Angiopoitin1 signaling to endothelial-Tie2 and angiocrine Tgfβ1 that impacts back in NPCs. This data brings new insights on how the neural and vascular compartment within the same organ cooperate during development and how angiocrine factors shape and guide CNS development.

Background

OPCs, which arise from NPCs during embryonic development [1], give rise to oligodendrocytes (OLs). OLs are the myelinating glial cells of the CNS which are necessary to insulate and provide metabolic support to axons, allows rapid saltatory conduction for electrical impulses and normal CNS function [2]. As such, impaired OL generation leads to demyelinating diseases as multiple sclerosis or periventricular leukomalacia [3]. Investigating the regulatory mechanisms leading to oligodendrocyte precursor cell (OPC) specification and differentiation is thus essential for understanding developmental oligodendrogenesis and for proposing new targets for the treatment of such disorders.

In the developing spinal cord (SC), most OPCs originate from the motor neuron (MN) progenitor domain (pMN), a restricted Olig2-expressing ventral NPC population which generates OPCs from embryonic day 12.5 (E12.5) in the mouse directed by the morphogenic activity of floor plate-derived sonic hedgehog (Shh) [4-6] (Fig. 1). Shh signaling is fine-tuned by other neural-derived signals (e.g. FGFs [7,8], TGFβ [9,10] and Notch ligands [11,12]), raising the question whether oligodendrogenesis requires additional signals that together with Shh induce OPC commitment. At the same time as NPCs proliferate and undergo differentiation the CNS is being vascularized [13]. Remarkably, blood vessels grow closely aligned to NPC domains without fully invading neurogenic areas [14,15]. By E12.5, when OPC specification begins, vessels are in close proximity to the pMN domain [14,16] (Fig. 1). While CNS vascularization is known to be regulated by signals derived from the neural compartment and to acquire organ-specific properties [13,17], remains unknown whether the vasculature

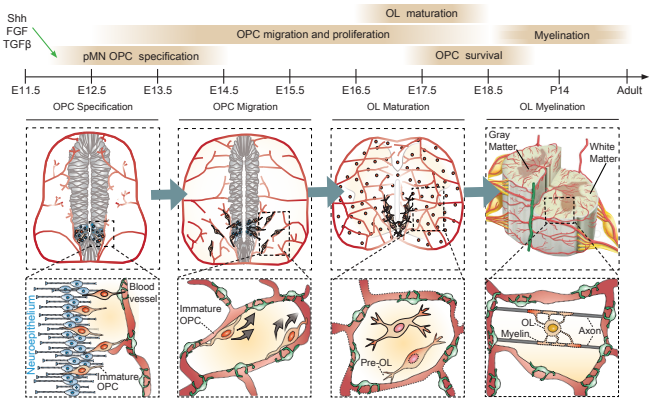

Figure 1: **OPCs associate with the vasculature during CNS development.** At midgestation, ventral neural progenitor cell domains are arranged along the neural tube dorso-ventral axis of spinal cord. The ventral motor neuron progenitor domain (in blue) commits to the oligodendrocyte lineage instructed by Shh signaling and other cues such as FGFs and TGFβ, specifying into OPCs (in orange) from E12.5[1] (OPC specification boxes). After specification, newly generated OPCs require the vasculature to migrate throughout the CNS and proliferate[42], while promoting angiogenesis[43] (OPC migration box). At their final destination, OPCs proliferate to expand the pool and, start to differentiate detaching from the vasculature into premyelinating oligodendrocytes (OL maturation box). Only afterwards and at around birth, pre-OLs mature into myelinating oligodendrocytes and myelinate target axons [30] (OL myelination box). FGF: Fibroblast, OPC: oligodendrocyte precursor cell, OL: Oligodendrocyte, pre-OL: premyelinating oligodendrocyte, Shh: Sonic Hedgehog, growth factor, TGFβ: Transforming growth factor beta.

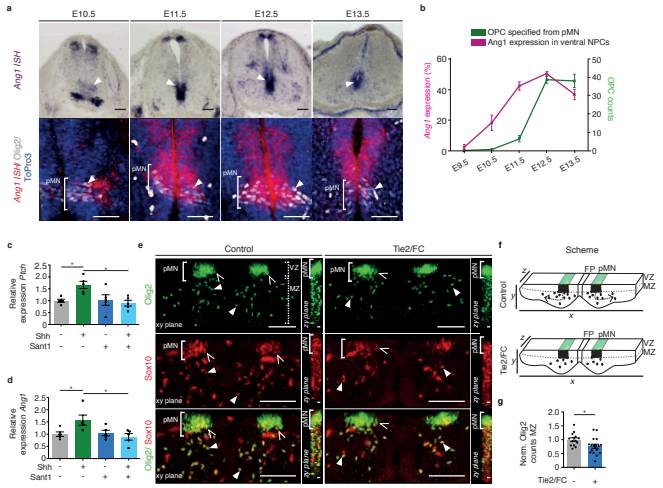

Figure 2: **Ang1 is expressed in SC NPCs and regulates OPC specification.**

(a) *Ang1 ISH* in transverse sections from E10.5 to E13.5 mouse embryos at brachial level (upper panels). Combined *Ang1 ISH* (pseudo-coloured in red) with Olig2 immunofluorescence (lower panels). Arrowheads point to *Ang1*$^{+}$ colocalization with Olig2^{+} pMN NPCs. Scale bar 50µm (lower) and 100µm (upper).

(b) Plot showing that Ang1 expression (% of the area of *Ang1* positive signal in ventral NPCs domains- left y-axis) sequentially overlaps with OPC specification (OPC counts – right y-axis) at the pMN between E9.5 till E13.5 (see Methods section for more details). Graphs show mean±SEM (Olig2 counts independent images from E9.5 n=5 from 1 embryo, E10.5 n=20 from 3 independent embryos, E11.5 n=16 from 2 independent embryos, E12.5 n=24 from 4 independent embryos, E13.5 n=15 from 4 independent embryos; Ang1 expression: E9.5 n=6, E10.5 n=8, E11.5 n=7, E12.5 n=14, E13.5 n=7 independent images from 2 independent embryos).

(c) and (d) Relative *Ptch* (c) and *Ang1* (d) expression in NSPs derived from E11.5 SC progenitors stimulated with recombinant Shh (500ng/mL) and/or Shh inhibitor Sant1 (150nM). Graphs show mean±SEM (n= 5 independent experiments; one-way ANOVA *Ptch* Control versus Shh *p=0.0391; Shh versus Shh+Sant1 *p=0.0142. *Ang1* Control versus Shh *p=0.0375; Shh+Sant1 *p=0.0242).

(e) Whole-mount SCs explants immunostained for Olig2 and Sox10 to detect OPCs (arrowheads) in the VZ and MZ after culturing in control (vehicle) or recombinant Tie2/FC (2µg/mL) in the y-x plane of Z-stacks images. On the right side of each image, an orthogonal projection is shown for the z-y plane of a Z-stack. Scale bar 100µm. Open arrowheads indicate OPCs in the pMN (VZ) and filled arrowheads in the MZ. Quantification in panel 1g.

(f) Scheme summarizing the phenotype of explants treated with recombinant Tie2/FC or in control conditions. The *z-y-x* planes are also depicted in order to illustrate the positioning of the cells. A scheme of explant preparation is also provided in Extended Data Fig. 2e.

(g) Quantification of the number of OPCs in the MZ (Olig2^{+}), normalized to vehicle treated explants. Analysis from panel 1e. Graphs show mean±SEM (control=13, Tie2/FC=17; 5 independent litters). Unpaired two-sided T-test, *p<0.0248.

responds to those signals by elongating and branching, or if they also signal back to the neural compartment. Moreover, the function that the developing vasculature might exert in NPCs during development, in particular during oligodendrogenesis, is largely unexplored.

Blood vessels are well recognized by performing their conventional function (transport of oxygen, nutrients, waste, cells, etc), however, recently they are also recognized as active orchestrators of organogenesis, tissue homeostasis and regeneration [18-20]. EC-derived paracrine (also known as angiocrine) factors can act on other cell types in their vicinity to influence their behavior. The Angiopoietin/Tie2 signaling system, a key regulator of vessel formation and homeostasis [21], also regulates the production of angiocrine signals [22]. Angiopoietins (Angs) are glycosylated secreted proteins that bind to the tyrosine kinase receptor Tie2 (also known as TEK) in ECs to promote EC survival, vessel stability and barrier function [21,23]. Ang1 expression has been described in different cell types including mural cells, fibroblasts, and neural cells and acts in a paracrine manner to activate its receptor [21]. Although limited *in vitro* studies have shown that Ang1/Tie2 signaling exerts neurovascular roles, it remains to be explored *in vivo* whether Ang1/Tie2 system participates in the neurovascular interface during CNS development.

Main results

Angiopoietin1 expression in the developing spinal cord correlates with OPC specification

In an attempt to better understand the expression of angiogenic factors in the developing mouse embryonic SC, we performed a temporal analysis of *Ang1* expression determined by *in situ* hybridization *(ISH)* (Fig. 2a). Between stages E10.5 and E13.5, *Ang1* was expressed by ventricular NPCs in a dynamic spatio-temporal manner (Fig. 2a). At E10.5, *Ang1* begins to be expressed by the ventral Olig2^{+} pMN and constitutes the most ventral progenitor domain expressing *Ang1* until at least E13.5 (Fig. 2a). The expression pattern of *Ang1* led us to explore whether its expression in NPC domains could be regulating NPC behaviour. Notably, the increase of *Ang1* transcript expression in ventral progenitors coincides with the process of OPC specification (Fig. 2b). Altogether, revealing a temporal correlation between OPC specification and *Ang1* expression during embryonic development, which prompted us to ask whether *Ang1* itself could have a regulatory role in OPC generation.

Endogenous Ang1 expression is controlled by Shh and regulates OPC specification ex vivo

One of the major regulators of OPC specification is Shh [5,24]. As Ang1 expression in astrocytes and fibroblasts is regulated by Shh [25,26], we questioned whether Shh could transcriptionally regulate Ang1 expression in SC NPCs. For this, we isolated NPCs from E11.5 wildtype SCs and cultured them as neurospheres (NSPs). The NSP cultures stimulated with recombinant Shh resulted in an upregulation of Shh target gene Ptch (Fig. 2c), as

well as *Ang1* (Fig. 2d). *Ang1* expression was indeed dependent on Shh signalling as the addition of the Shh pathway inhibitor Sant1 [27] abolished its induction (Fig. 2d).

To test the hypothesis that Ang1 signalling might regulate OPC development, we used ex vivo cultures of E11.5 mouse embryo SC explants (in an open-book preparation [28]), in which it is possible to analyse OPC specification and migration from the pMN domain to the MZ [29] (Fig. 2f). We treated the explants with a recombinant soluble Tie2 receptor (Tie2/FC), which traps *Ang1* thus blocking endogenous Ang1. OPCs (Olig2$^+$) migrating to the MZ after 24h were reduced in Tie2/FC treated explants compared to vehicle-treated ones (Fig. 2e-g). Sox10 is one of the earliest transcription factors expressed by pMN NPCs in the ventricular zone (VZ) when committed to the OL lineage [3,30,31], and we found no accumulation of specified OPCs (Olig2$^+$ Sox10$^+$ double-positive cells) in the pMN or its vicinity (Fig. 2e), suggesting that migration of specified OPCs from the pMN was not affected. Notably, in the pMN, while comparable numbers of Olig2+ cells were seen, less Sox10+ NPCs were observed (Fig. 2e), suggesting that *Ang1* signalling from NPCs was required for OPC specification. In summary, these results indicate that *Ang1* expression in NPCs is regulated by Shh and that *Ang1* is required (at least partially) for Shh-induced OPC specification ex vivo.

CNS-derived Ang1 regulates OPC specification in vivo

Due to early embryonic lethality of *Ang1* null embryos [32-34], we generated a CNS *Ang1* conditional knock-out mouse line by crossing *Ang1* floxed mice (*Ang1* fl/fl, kindly provided by Susan E. Quaggin [33]) with a Nestin:Cre driver line [35] that targets all neural progenitors (Fig. 3a). Using these embryos, we studied OPC specification by assessing the number of newly specified OPCs in the VZ and migrating OPCs localized in the MZ as previously reported [31]. At E12.5, *Ang1* ablated embryos present a strong reduction in OPCs (Olig2$^+$ Sox10$^+$ double-positive cells) in the VZ and MZ at brachial level (Fig. 3b, c). The total number of Olig2$^+$ cells in the pMN was similar between Ang1 fl/fl and Ang1 fl/fl$^{Nestin:Cre}$ animals (Fig. 3d), resulting in a decreased ratio of VZ OPCs in Ang1 fl/fl$^{Nestin:Cre}$ embryos (Fig. 3e). Altogether, this suggests that the reduced OPC number was due to a failure in OPC specification and not to a defect in cell death or proliferation of neural progenitors in general.

OPCs arise in the developing SC from the pMN domain (Olig2$^+$). As this domain was the most ventral NPC domain expressing *Ang1* during SC development (Fig. 2a), we next asked whether the exclusive deletion of pMN-derived *Ang1* would also result in reduced OPC specification. Thus, we genetically deleted *Ang1* in Olig2$^+$ pMN-NPCs by crossing *Ang1* fl/fl with Olig2:Cre mice

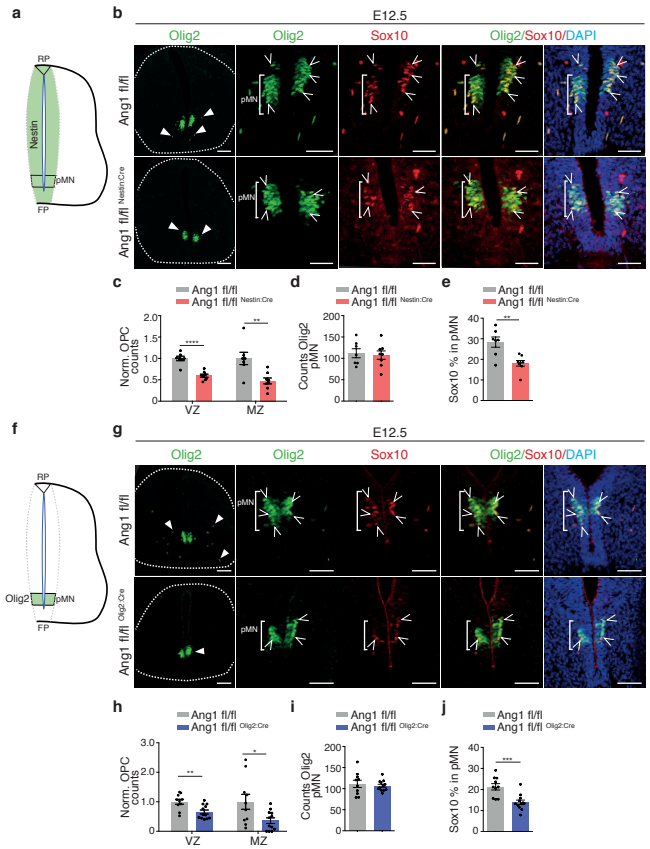

Figure 3: **NPC-derived Ang1 regulates OPC specification.**

(a) Scheme showing Nestin expression in SC-NPCs to illustrate that Nestin:Cre driver mediates Ang1 deletion in all NPCs.

(b) Images of transverse sections at brachial level of Ang1 fl/fl (control) and Ang1 fl/fl$^{Nestin:Cre}$ E12.5 embryos. Left images: entire SC immunostained with Olig2. Right images: pMN domain immunostained for Olig2 and Sox10. Bracket: pMN; open arrowheads indicate OPCs in the pMN (VZ) and filled arrowheads in the MZ. Scale bars 100µm (left images) and 50µm (images of pMN).

(c) Quantification of OPCs in the VZ and MZ of Ang1 fl/fl and Ang1 fl/fl$^{Nestin:Cre}$, normalized to control littermates.

(d) Analysis of the number of Olig2$^+$ progenitors in the pMN.

(e) Ratio of VZ Sox10$^+$ cells within the total number of Olig2$^+$ pMN cells. Graphs show mean±SEM (Ang1 fl/fl =7, Ang1 fl/fl$^{Nestin:Cre}$ =8 of 4 independent litters). Unpaired two-sided T-test (VZ ****p<0.0001, MZ **p=0.0098, Sox10% **p=0.0051).

(f) Scheme showing Olig2 expression in SC pMN to illustrate that Olig2:Cre driver mediates Ang1 deletion only in pMN and its progeny.

(g) Images of transverse sections at brachial level of Ang1 fl/fl and Ang1 fl/fl$^{Olig2:Cre}$ E12.5 embryos. Left images: entire SC immunostained with Olig2. Right images: pMN domain immunostained for Olig2 and Sox10. Bracket: pMN; open arrowheads indicate OPCs in the pMN and filled arrowheads in the MZ. Scale bars 100µm (left images) and 50µm (images of pMN).

(h) Quantification of OPCs in the VZ and MZ of Ang1 fl/fl and Ang1 fl/fl$^{Olig2:Cre}$.

(i) Analysis of the number of Olig2$^+$ progenitors in the pMN.

(j) Ratio of VZ Sox10$^+$ cells within the total number of Olig2$^+$ pMN progenitor cells. Graphs show mean±SEM (Ang1 fl/fl =10, Ang1 fl/fl$^{Olig2:Cre}$ =12 of 3 independent litters). Unpaired two-sided T-test. (VZ **p=0.0050; MZ *p=0.0375; Sox10% ***p=0.0009). Dashed lines mark the perimeter of the SC

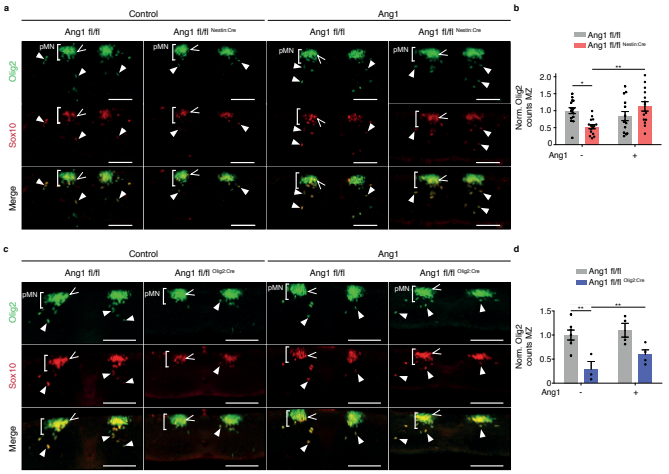

Figure 4: **Exogenous Ang1 rescues OPC specification defects in Ang1 fl/fl$^{Nestin:Cre}$ and Ang1 fl/fl$^{Olig2:Cre}$ embryos *ex vivo*.**

(a) 100µm transverse sections of Ang1 fl/fl and Ang1 fl/fl$^{Nestin:Cre}$ SC explants immunostained for Olig2 and Sox10 to detect OPCs in the VZ (open arrowheads) and MZ (filled arrowheads) after culturing with control (vehicle) or recombinant Ang1 300 ng/mL for 24h. Scale bar 100µm.

(b) Quantification of the number of OPCs in the MZ (Olig2$^+$), normalized to control (Ang1 fl/fl) untreated explants. Mean±SEM (Control; Ang1 fl/fl =15, +Ang1; Ang1 fl/fl =14, Control; Ang1 fl/fl$^{Nestin:Cre}$ =15, +Ang1; Ang1 fl/fl$^{Nestin:Cre}$ =14 of 6 independent litters). Two-way ANOVA (Control;Ang1 fl/fl versus Control; Ang1 fl/fl$^{Nestin:Cre}$ *p=0.0164; Control; Ang1 fl/fl$^{Nestin:Cre}$ versus +Ang1; Ang1 fl/fl$^{Nestin:Cre}$ **p=0.0015).

(c) 100µm transverse sections of Ang1 fl/fl and Ang1 fl/fl$^{Olig2:Cre}$ SC explants immunostained for Olig2 and Sox10 to detect OPCs in the VZ (open arrowheads) and MZ (filled arrowheads) after culturing with control (vehicle) or recombinant Ang1 300ng/mL for 24h. Scale bar 100µm.

(d) Quantification of the number of OPCs in the MZ (Olig2$^+$), normalized to control (Ang1 fl/fl) untreated explants. Graph show mean±SEM (Control; Ang1 fl/fl=7, +Ang1; Ang1fl/fl=4, Control; Ang1 fl/fl$^{Olig2:Cre}$ =3, +Ang1; Ang1 fl/fl$^{Olig2:Cre}$ =4 of 4 independent litters). Two-way ANOVA (Control; Ang1 fl/fl versus Control; Ang1 fl/fl$^{Olig2:Cre}$ **p=0.0093; Control; Ang1 fl/flOlig2:Cre versus +Ang1; Ang1 fl/flOlig2:Cre **p=0.0074).

[36] (Fig. 3f). Similar as in Ang1 fl/fl$^{Nestin:Cre}$, E12.5 Ang1 fl/fl$^{Olig2:Cre}$ embryos showed less OPC numbers in the MZ and in the VZ at brachial level (Fig. 3g-j).

To verify that the observed OPC reduction was specific to *Ang1* loss-of-function, we aimed to rescue the phenotype, utilizing SC *ex vivo* explant cultures and applying exogenous recombinant *Ang1*. Similar as observed *in vivo*, *Ang1* fl/fl$^{Nestin:Cre}$ and Ang1 fl/fl$^{Olig2:Cre}$ resulted in reduced OPC counts in the MZ when compared to control littermates. Conversely, addition of exogenous *Ang1* rescued the phenotype and increased the number of newly-specified OPCs in Ang1 fl/fl$^{Nestin:Cre}$ and *Ang1* fl/fl$^{Olig2:Cre}$ SC explants (Fig. 4a, b and Fig. 4c, d, respectively).

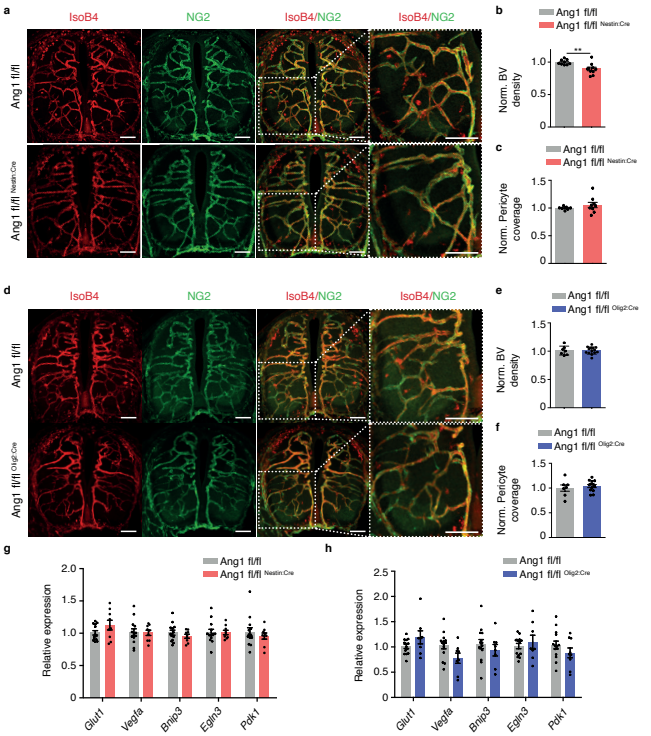

Figure 5: **Reduced OPC specification in Ang1 deficient embryos cannot be explained by morphological vascular defects.**

(a) Transverse thick sections of E12.5 Ang1 fl/fl (control) and Ang1 fl/fl$^{Nestin:Cre}$ stained with IsoB4 to visualize blood vessels and NG2 for pericytes. Scale bar 100µm and inset 50µm.

(b) Quantification of blood vessel (BV) density in Ang1 fl/fl and Ang1 fl/fl$^{Nestin:Cre}$ and normalized to control (Ang1 fl/fl) littermates. Graphs show mean±SEM (Ang1 fl/fl=9, Ang1 fl/fl$^{Nestin:Cre}$ =10, of 3 independent litters). Unpaired two-sided T-test (BV density **p=0.0041).

(c) Quantification of pericyte coverage of blood vessels, expressed as the percentage of pericyte density with respect to the vascular density in each cross-section of Ang1 fl/fl$^{Nestin:Cre}$ and normalized to control (Ang1 fl/fl) littermates. Graphs show mean±SEM (Ang1 fl/fl=9, Ang1 fl/fl$^{Nestin:Cre}$ =10, of 3 independent litters). Unpaired two-sided T-test.

(d) Transverse thick sections of E12.5 Ang1 fl/fl (control) and Ang1 fl/fl$^{Olig2:Cre}$ stained with IsoB4 to visualize blood vessels and NG2 for pericytes. Scale bar 100µm and inset 50µm.

(e) Quantification of blood vessel (BV) density in Ang1 fl/fl and Ang1 fl/fl$^{Olig2:Cre}$ and normalized to control (Ang1 fl/fl) littermates. Graphs show mean±SEM (Ang1 fl/fl=7, Ang1 fl/fl$^{Olig2:Cre}$ =14, from 2 independent litters)

(f) Quantification of pericyte coverage of blood vessels, expressed as the percentage of pericyte density with respect to vascular density in each cross-section of Ang1 fl/fl$^{Olig2:Cre}$ and normalized to control (Ang1 fl/fl) littermates. Graphs show mean±SEM (Ang1 fl/fl=7, Ang1 fl/fl$^{Olig2:Cre}$ =13, from 2 independent litters). Unpaired two-sided T-test.

(g) and (h) Relative expression of hypoxia response genes *Glut1*, *Vegfa*, *Bnip3*, *Egln3*, and *Pdk1* from the neural compartment (CD31- negative selection) from Ang1 fl/fl or Ang1 fl/fl$^{Nestin:Cre}$ (g) and Ang1 fl/fl or Ang1 fl/fl$^{Olig2:Cre}$ (h) E12.5 SCs. Graphs show mean±SEM (Ang1 fl/fl=13, Ang1 fl/fl$^{Nestin:Cre}$=9, from 3 independent litters; Ang1 fl/fl=14, Ang1 fl/fl$^{Olig2:Cre}$=8, from 4 independent litters). Unpaired two-sided T-test.

Reduced OPC specification is not caused by differences in blood vessel density or hypoxia.

As *Ang1* best known function is the regulation of blood vessel formation and maturation [21], we questioned whether the observed OPC specification defect could be a consequence of impaired vascularization. While Ang1 fl/fl$^{Nestin:Cre}$ embryos presented a mild reduction in SC blood vessel density (Fig. 5a, b), *Ang1* fl/fl$^{Olig2:Cre}$ did not reveal any difference (Fig. 5d, e). Moreover, no differences were observed in pericyte-blood vessel coverage in none of Ang1-deficient embryos (Fig. 5c, f). Also, no functional defects were observed in any of the transgenic lines as the expression of classical hypoxia-induced target genes (*Glut1, Vegfa, Bnip3, Egln3 and Pdk1*) in the isolated neural compartment of E12.5 SCs was not different between *Ang1*-ablated embryos and their corresponding control littermates (Fig. 5g, h). The lack of hypoxia and the fact that no differences in blood vessel density were observed in *Ang1* fl/fl$^{Olig2:Cre}$ embryos (while those embryos presented an OPC specification defect) suggest that the observed OPC specification defects were not a consequence of vascular malfunction.

Tie2 is exclusively expressed in blood vessels

One potential mechanism of *Ang1*-mediated effects to regulate OPC specification could be that Ang1 signals directly to NPCs to induce specification. For this, *Tie2*, the cognate Ang1 receptor, should be expressed by NPCs. We analysed *Tie2* expression in the developing SC by ISH from E11.5 to E13.5 and found that *Tie2* mRNA transcripts were only detected in blood vessel-like structures (Fig. 6a). Next, we used two different genetic approaches to confirm *Tie2* localization to the endothelium: mTmG$^{Tie2:CreERT2}$, where *Tie2*-driven recombination leads to GFP expression, and Tie2:GFP mice [37]. In both cases, GFP signal was restrained to CD31$^+$ ECs (Fig. 6b and Fig. 6c). Finally, Tie2

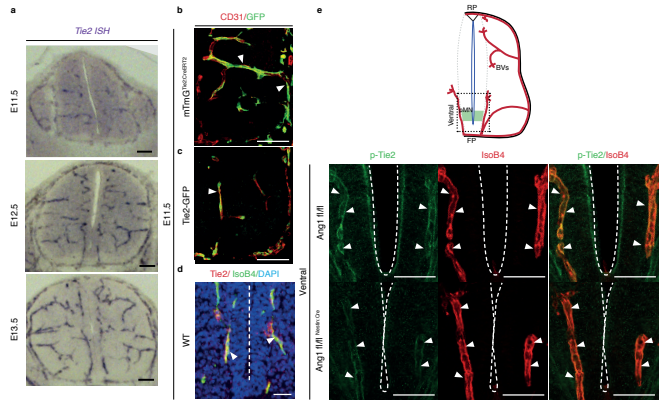

Figure 6: **Tie2 is exclusively expressed by blood vessels.**

(a) *ISH* for Tie2 in transverse sections of wild-type embryos between E11.5 and E13.5. Scale bar 100µm.

(b) Transverse section of tamoxifen-inducible mTmG$^{Tie2:CreERT2}$ E11.5 embryo, showing Tie2-driven recombination and consequently GFP expression (green), co-localizing with CD31$^+$ blood vessels (pseudo-coloured in red). Scale bar 50µm.

(c) Transverse section of transgenic Tie2-GFP embryo (E11.5) showing GFP (green) expression in CD31$^+$ blood vessels (red). Scale bar 50µm.

(d) Immunofluorescence for Tie2 and IsoB4$^+$ blood vessels in E11.5 wild-type embryo transverse section. Scale bar 25µm.

(e) Scheme of the ventral region of the SC including the pMN and adjacent blood vessels (upper panel). Phospho-Tie2 (p-Tie2) staining combined with the blood vessel marker IsoB4 in Ang1 fl/fl$^{Nestin:Cre}$ and control littermate in blood vessels adjacent to pMN (lower panels). Note the decreased Tie2 phosphorylation in vessels proximal to the VZ. Scale bar 50µm.

All data is representative from at least 3 independent experiments.

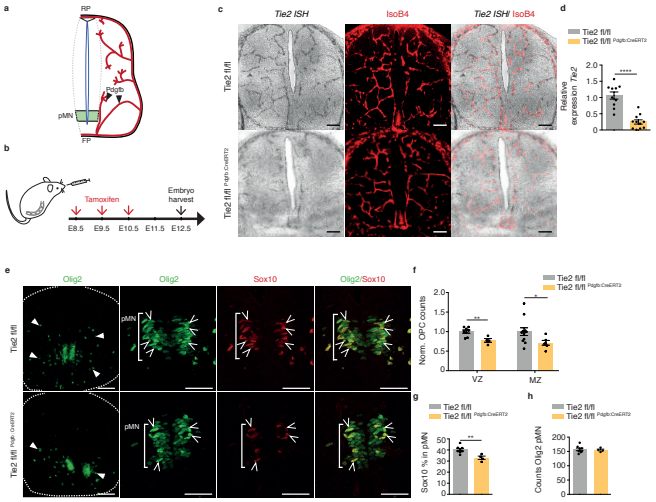

Figure 7: **Endothelial Tie2 signalling is required for OPC specification.**

(a) Scheme of Pdgfb expression in ECs of blood vessels to illustrate that Pdgfb:CreERT2 driver mediates Tie2 deletion in ECs.

(b) Scheme protocol of tamoxifen administration of Tie2 fl/fl$^{Pdgfb:\ CreERT2}$ pregnant females and embryo harvest for analysis.

(c) Tie2 ISH in E12.5 Tie2 fl/fl and Tie2 fl/fl$^{Pdgfb:\ CreERT2}$ and combined with IsoB4 staining. Scale bar 100µm.

(d) Relative expression of Tie2 mRNA in isolated ECs from E12.5 Tie2 fl/fl (control) and Tie2 fl/fl$^{Pdgfb:CreERT2}$ SCs. Graph show mean±SEM (Tie2 fl/fl =10, Tie2 fl/fl$^{Pdgfb:\ CreERT2}$ =11, from 3 independent litters). Unpaired two-sided T-Test (***p<0.0001).

(e) Images of transverse sections at brachial level of Tie2 fl/fl and Tie2 fl/fl$^{Pdgfb:\ CreERT2}$ E12.5 embryos. Left images: entire SC immunostained with Olig2. Right images: pMN domain immunostained for Olig2 and Sox10. Bracket: pMN; open arrowheads indicate OPCs in the pMN and filled arrowheads in the MZ. Scale bars 100µm (left images) and 50 µm (images of pMN).

(f) Quantification of OPCs in the VZ (Tie2 fl/fl =8, Tie2 fl/fl$^{Pdgfb:\ CreERT2}$ =4 of 2 independent litters) and MZ (Tie2 fl/fl =11, Tie2 fl/fl$^{Pdgfb:\ CreERT2}$ =6 of 2 independent litters) of Tie2 fl/fl and Tie2 fl/fl$^{Pdgfb:\ CreERT2}$, normalized to controls.

(g) Ratio of VZ Sox10$^+$ cells within the total number of Olig2$^+$ pMN progenitor cells (Tie2 fl/fl =8, Tie2 fl/fl$^{Pdgfb:\ CreERT2}$ =4 of 2 independent litters).

(h) Analysis of the number of Olig2+ progenitors in the pMN (Tie2 fl/fl =8, Tie2 fl/fl$^{Pdgfb:\ CreERT2}$ =4 of 2 independent litters). Graphs show mean±SEM. Unpaired two-sided T-test (VZ **p=0.0086; MZ*p=0.0264; Sox10% **p=0.0068).

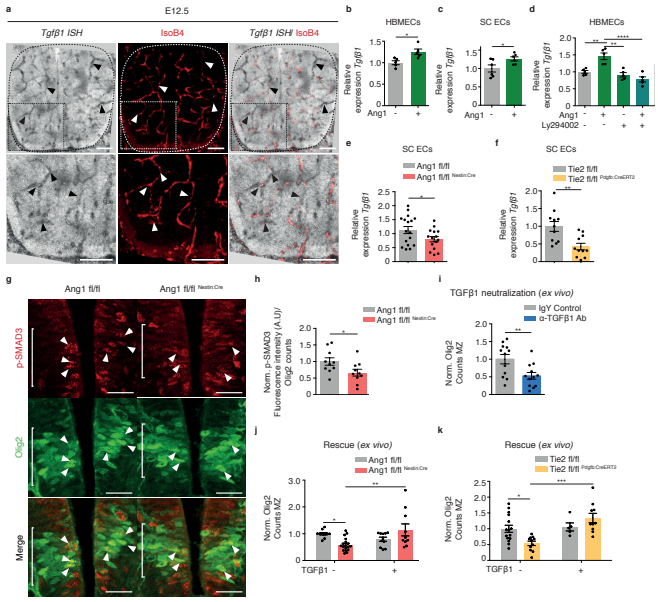

Figure 8: **EC-derived TGFβ1 is regulated by Tie2 signalling and required for proper OPC specification.**

(a) *Tgfβ1* ISH in E12.5 wild-type embryo and stained for blood vessels (IsoB4+) (arrowheads show localization of *Tgfβ1* mRNA in the vasculature). Scale bar 100µm.

(b) and (c) Relative expression of *Tgfβ1* transcript of human brain microvascular ECs (HBMECs) (b) and isolated E12.5 wild-type SC-ECs (c) upon control or recombinant Ang1 stimulation. Graphs show mean±SEM (b), n= 5 independent experiments), unpaired two-sided T-test *p=0.0146, (c), n= 6 indpendent experiments, unpaired two-sided T-test *p=0.0479.

(d) Relative expression of *Tgfβ1* transcript in human brain microvascular ECs (HBMECs) treated with vehicle (DMSO), recombinant Ang1 and/or Akt/PI3K inhibitor Ly294002. Graphs show mean±SEM (n= 5 independent experiments). One-way ANOVA, Control versus +Ang1 **p=0.0077; +Ang1 versus +Ly294002 **p=0.0012; +Ang1 versus +Ang1+Ly294002 ****p<0.0001.

(e) and (f) Relative expression of *Tgfβ1* mRNA in CD31+ ECs sorted from Ang1 fl/fl and Ang1 fl/fl$^{Nestin:Cre}$ E12.5 SCs (e) and Tie2 fl/fl and Tie2 fl/fl$^{Pdgfb:CreERT2}$ SCs (f).

Graphs show mean±SEM (Ang1 fl/fl=17, Ang1 fl/fl$^{Nestin:Cre}$=15, from 4 independent litters, Unpaired two-sided T-test, *p=0.0495 and Tie2fl/fl =11, Tie2fl/fl $^{Pdgfb:CreERT2}$ =11, from 3 independent litters, Unpaired two-sided T-test, **p=0.0033).

(g) Co-immunostaining for phospho-SMAD3 (p-SMAD3) and Olig2 at the pMN level of E12.5 Ang1 fl/fl and Ang1 fl/fl$^{Nestin:Cre}$ embryo transverse section. Arrowheads show Olig2+ pSMAD3+ double-positive cells. Scale bar 25µm.

(h) Quantification of p-SMAD3 fluorescence intensity per Olig2$^+$ cell counts in the pMN of Ang1 fl/fl and Ang1 fl/fl$^{Nestin:Cre}$ normalized to control littermates. Graph show mean±SEM (Ang1 fl/fl =10, Ang1 fl/fl$^{Nestin:Cre}$ =10, of 3 independent litters). Unpaired two-sided T-test, *p=0.040. A.U= Arbitrary Units

(i) Quantification of the number of OPCs in the MZ (Olig2$^+$) from wild-type E11.5 explants treated with α-TGFβ1 blocking antibody (α-TGFβ1 Ab) or vehicle (IgY Control) (5µg/mL) for 24 h, values are normalized to control treated explants. Graphs show mean±SEM (IgY control=12, α-TGFβ1 Ab=12; 3 independent litters). Unpaired two-sided T-test, **p=0.0088.

(j) Quantification of OPC number in the MZ (Olig2$^+$) of Ang1 fl/fl and Ang1 fl/flNestin:Cre SCs explants after culturing with control (vehicle) or recombinant TGFβ1 50ng/mL, normalized to control (vehicle of Ang1 fl/fl). Graph show mean±SEM (Control; Ang1 fl/fl =11, +TGFβ1; Ang1 fl/fl =10, Control; Ang1 fl/fl$^{Nestin:Cre}$ =18, + TGFβ1; Ang1 fl/fl$^{Nestin:Cre}$ =12 of 7 independent litters). Two-way ANOVA, Control; Ang1 fl/fl versus Control; Ang1 fl/fl$^{Nestin:Cre}$ *p=0.0449; Control; Ang1 fl/fl$^{Nestin:Cre}$ versus + TGFβ1; Ang1 fl/flNestin:Cre **p=0.0029.

(k) Quantification of the number of OPCs in the MZ (Olig2$^+$) of Tie2 fl/fl and Tie2 fl/fl$^{Pdgfb:CreERT2}$ SCs explants after culturing with control (vehicle) or recombinant TGFβ1 50ng/mL, normalized to control (vehicle of Tie2 fl/fl). Graph show mean±SEM (Control; Tie2 fl/fl =15, + TGFβ1; Tie2 fl/fl =11, Control; Tie2 fl/fl $^{Pdgfb:CreERT2}$ =5, + TGFβ1; Tie2 fl/fl $^{Pdgfb:CreERT2}$ =10 of 5 independent litters). Two-way ANOVA, Control; Tie2 fl/fl versus Control; Tie2 fl/fl $^{Pdgfb:CreERT2}$ *p=0.0278; Control; Tie2 fl/fl $^{Pdgfb:CreERT2}$ versus + TGFβ1; Tie2 fl/fl $^{Pdgfb:CreERT2}$ ***p=0.0002.

immunostaining also showed *Tie2* expression confined to the vasculature (Fig. 6d).

Endothelial Tie2 regulates OPC specification

The above-mentioned results pointed towards a mechanism involving the vasculature, comprising Ang1 binding to EC-Tie2, and inducing a response in the vasculature. Therefore, we reasoned that if Ang1 is activating Tie2 in blood vessels, its activation should be reduced in Ang1-deficient SCs. Consistent with this hypothesis, phospho-Tie2 (p-Tie2) signal was reduced in blood vessels in the ventral SC region of Ang1 fl/fl$^{Nestin:Cre}$ compared to control littermates (Fig. 6e).

Next, we tested the hypothesis that endothelial-derived cues triggered by Ang1-Tie2 signalling may promote OPC specification. For this, we analysed OPCs in transgenic mouse embryos genetically lacking Tie2 in ECs [38] (Tie2 fl/fl$^{Pdgfb:CreERT2}$) (Fig. 7a). To overcome early embryonic lethality, we induced *Tie2* deletion by Tamoxifen delivery to pregnant females from E8.5 to E10.5 and analysed embryos at E12.5 (Fig. 7b). Analysis of *Tie2* expression by ISH and by qPCR in primary isolated ECs from embryonic SCs revealed that Tie2 was efficiently deleted in *Tie2* fl/fl$^{Pdgfb:CreERT2}$ embryos (Fig. 7c, d).

Remarkably, Tie2 fl/fl$^{Pdgfb:CreERT2}$ embryos presented an OPC specification-phenotype similar to the one observed in embryos in which Ang1 was ablated from NPCs (Fig. 7e-h). Consistent also with the phenotype seen in NPC *Ang1*-deficient embryos, no accumulation of already specified OPCs in the pMN was observed in Tie2 fl/fl$^{Pdgfb:CreERT2}$ embryos (Fig. 7e), suggesting that migration of specified OPCs is not impaired.

Altogether these data indicate that Tie2 signalling in SC ECs is

required for proper OPC specification. As blood vessel density was not affected, these data further highlight a potential angiocrine mechanism that could signal back to NPCs to induce OPC specification.

EC-derived TGFβ1 is regulated by Tie2 signalling and required for normal OPC specification

Previous reports have shown that TGFβ signalling is required during OPC development and CNS myelination. Notably, those reports were based on the deletion of TGFβ receptors in NPCs, or its intracellular signalling effector SMAD3 [9,10,39], without identifying/confirming the cellular source of the ligands. We found that Tgfβ1 is expressed in ECs at the developmental time points when OPC specification occurs (Fig. 8a). Similar as in liver ECs, where Tie2 activation regulates Tgfβ1 expression during liver regeneration [22], we found that Tgfβ1 expression was upregulated in human brain microvascular ECs (HBMECs) and primary ECs isolated from SCs of E12.5 embryos upon activation of Ang1/Tie2 signalling (Fig. 8b, c). In line, blockade of the Tie2-induced intracellular signalling cascade by pharmacologically inhibiting the AKT/PI3K pathway with Ly294002 abolished the upregulation of Tgfβ1 transcript upon Ang1 stimulation (Fig. 8d). Consistently, Tgfβ1 expression was significantly reduced in ECs isolated from SCs of E12.5 Ang1 fl/fl$^{Nestin:Cre}$ and Tie2 fl/fl$^{Pdgfb:CreERT2}$ (Fig. 8e, f).

We reasoned that if EC-derived TGFβ1 is downstream of Ang1/Tie2 signalling, and it is required for OPC specification, its signalling should be decreased in NPCs of *Ang1*-deficient embryos. Indeed, quantitative analysis of the activation of the TGFβ1 intracellular effector, SMAD3 [40], in pMN cells showed reduced pSMAD3^{+}Olig2^{+} progenitors in Ang1 fl/fl$^{Nestin:Cre}$ embryos (Fig. 8g,h). Moreover, neutralization of endogenous TGFβ1 (using a functional TGFβ1-blocking antibody) in SC explants from WT embryos resulted in reduced OPC specification, suggesting that EC-derived TGFβ1 is required in this process (Fig 8i). Consistently, recombinant TGFβ1 as compared to vehicle could rescue the OPC specification phenotype utilizing the SC explant culture system in both Ang1 fl/fl$^{Nestin:Cre}$ and Tie2 fl/fl^{PdgfbCreERT2} genotypes (Fig. 8j, k).

Collectively, these results identify TGFβ1 as an EC-derived angiocrine signal, which is regulated by Ang1/Tie2 signalling, and that is required for proper OPC specification.

Discussion and conclusions

This study identifies a unique mechanism of bi-directional intercellular communication between the neural and the vascular compartment of the developing CNS, where the vasculature instructs and controls oligodendrogenesis via angiocrine signaling. Our data propose a collaborative model in which neural cells and ECs instruct each other to achieve the final goal of inducing OPC specification. This involves (1) floor plate-derived Shh, which signals to NPCs to regulate Ang1 expression; (2) NPC-derived Ang1 signals then to ECs, activating Tie2 (3) and induces TGFβ1 expression (4); (5) EC-derived TGFβ1 acts as a paracrine signal and signals back to NPCs of the pMN domain and activates SMAD-3 (6) to induce their specification towards OPCs (8) (Figure 9).

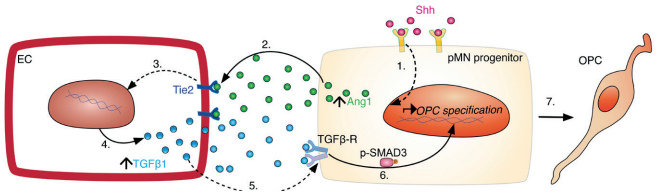

Figure 9: **Model of bi-directional NPC-EC communication regulating OPC specification.**
(a) Step-by-step model of the identified NPC-EC bidirectional crosstalk required for OPC specification. **1 and 2**. Floor plate/Notochord-derived Shh transcriptionally regulates Ang1 expression in NPCs. 3. NPC-derived Ang1 produced binds and activates Tie2 in ECs. **4 and 5**. Tie2 activation triggers Tgfβ1 transcriptional upregulation in ECs. **6**. Tgfβ1, signals back to pMN NPCs inducing phosphorylation of its intracellular effector SMAD3. 7. NPCs are induced to specify their fate to OPCs.

Notochord and floor plate-derived Shh acts as a long-range morphogen to direct SC morphogenesis by organizing the patterning of ventral SC progenitor domains and their specification towards different neuronal and glia subclasses [1,41]. Remarkably, in this study we show that Shh does not only recruit the neural compartment to orchestrate its action but that it also engages the growing vasculature to control OPC specification, thus synchronizing both the nervous and the vascular system. Shh do so in sequential steps, first it induces Ang1 expression in NPCs so that Ang1 can then act on ECs to induce an angiocrine response which later signals back to pMN-NPCs. Our data not only indicates that different cellular compartments of the CNS tightly communicate but also broadens the conventional view of Shh as a morphogen as it suggests that the response of the vasculature needs to be considered for the interpretation of Shh-mediated effects.

Recent evidence demonstrate that the vasculature is emerging as an active regulator of tissue formation, organ function, and regeneration [18,20]. However, little is known of the vasculature role in instructing cell fate specification during CNS development. In this study, we show that activation of an EC angiocrine response is crucial for instructing pMN-NPCs to specify their fate towards OPCs. We identify TGFβ1, expressed by ECs, as an angiocrine molecule that is regulated upon the activation of the Ang1/Tie2 signaling axis and that is required for OPC specification. Remarkably, a role for TGFβ signaling in OPC specification *in vivo* was proposed. However, our data thus adds further knowledge to this regulation as we identify that ECs are a source of TGFβ1 and that this is required for OPC specification. The three transgenic mouse lines analyzed showed impaired OPC specification. Interestingly, in Ang1 fl/fl$^{Nestin:Cre}$ mice, where Ang1 was deleted in whole CNS, presented defects in OL differentiation and maturation, suggesting that a cross-talk with the vasculature necessary for OPC specification, via Ang1/Tie2 signaling or indirectly via other factors regulated by Ang1 and/

or Tie2. Thus, suggesting that this signaling might not by uni-directional (OPC to vessel, or vessel to OPC) but bi-directional. However, the mechanisms of the bi-directional cross talk for differentiation and maturation remain to be determined.
Elucidating these intercellular mechanisms is needed to better understand the pathophysiological mechanisms of demyelinating disorders.

Acknowledgements

First of all, I would like to acknowledge all the people that participated and contributed for making this study possible. I would like to thank all co-authors whose team work was instrumental for the project's development and completion. I am very grateful for their tremendous support, hard work, valuable discussions and suggestions.
I am very grateful with my supervisor Prof. Dr. Carmen Ruiz de Almodóvar for encouraging and guiding me during my Ph.D. and Postdoc which prepare me for my next career steps and her enormous support, specially these last years. I thank her for her always valuable advice, observations and opinions that continuously kept me motivated.
Many thanks to all Ruiz lab members who made of the Ruiz lab a wonderful working environment and with who the lab was a place where I truly enjoyed to develop scientifically and personally. Thank you for all the discussions and constructive comments, and specially for the "hand" when I needed help.
Finally, I would like to thank the Werner Risau Prize committee and the DGZ for recognizing this work with the prestigious Werner Risau Prize. I am deeply honored and humbly thankful to be part of the vascular biology community.
This article was published in Nature Neuroscience. Paredes, I., Vieira, J.R., Shah, B. Ramunno, C.F.,Dyckow, J., Adler, H., Richter, M., Schermann, G., Giannakouri, E., Schirmer, L., Augustin, H.G., and Ruiz de Almodóvar, C. Oligodendrocyte precursor cell specification is regulated by bidirectional neural progenitor–endothelial cell crosstalk. *Nat Neurosci* **24**, 478–488 (2021). https://doi.org/10.1038/s41593-020-00788-z.

References

1 Rowitch, D. H. Glial specification in the vertebrate neural tube. *Nat Rev Neurosci* **5**, 409-419, doi:10.1038/nrn1389 (2004).
2 Simons, M. & Nave, K. A. Oligodendrocytes: Myelination and Axonal Support. *Cold Spring Harb Perspect Biol* **8**, a020479, doi:10.1101/cshperspect.a020479 (2015).
3 Fancy, S. P., Chan, J. R., Baranzini, S. E., Franklin, R. J. & Rowitch, D. H. Myelin regeneration: a recapitulation of development? *Annu Rev Neurosci* **34**, 21-43, doi:10.1146/annurev-neuro-061010-113629 (2011).
4 Orentas, D. M., Hayes, J. E., Dyer, K. L. & Miller, R. H. Sonic hedgehog signaling is required during the appearance of spinal cord oligodendrocyte precursors. *Development* **126**, 2419-2429 (1999).
5 Yu, K., McGlynn, S. & Matise, M. P. Floor plate-derived sonic hedgehog regulates glial and ependymal cell fates in the developing spinal cord. *Development* **140**, 1594-1604, doi:10.1242/dev.090845 (2013).
6 Zhou, Q. & Anderson, D. J. The bHLH transcription factors OLIG2 and OLIG1 couple neuronal and glial subtype specification. *Cell* **109**, 61-73 (2002).
7 Farreny, M. A. et al. FGF signaling controls Shh-dependent oligodendroglial fate specification in the ventral spinal cord. *Neural development* **13**, 3, doi:10.1186/s13064-018-0100-2 (2018).
8 Vallstedt, A., Klos, J. M. & Ericson, J. Multiple dorsoventral origins of oligodendrocyte generation in the spinal cord and hindbrain. *Neuron* **45**, 55-67, doi:10.1016/j.neuron.2004.12.026 (2005).
9 Dias, J. M., Alekseenko, Z., Applequist, J. M. & Ericson, J. Tgfbeta signaling regulates temporal neurogenesis and potency of neural stem cells in the CNS. *Neuron* **84**, 927-939, doi:10.1016/j.neuron.2014.10.033 (2014).
10 Dutta, D. J. et al. Combinatorial actions of Tgfbeta and Activin ligands promote oligodendrocyte development and CNS myelination. *Development* **141**, 2414-2428, doi:10.1242/dev.106492 (2014).
11 Rabadan, M. A. et al. Jagged2 controls the generation of motor neuron and oligodendrocyte progenitors in the ventral spinal cord. *Cell Death Differ* **19**, 209-219, doi:10.1038/cdd.2011.84 (2012).
12 Cui, X. Y. et al. NB-3/Notch1 pathway via Deltex1 promotes neural progenitor cell differentiation into oligodendrocytes. *J Biol Chem* **279**, 25858-25865, doi:10.1074/jbc.M313505200 (2004).
13 Paredes, I., Himmels, P. & Ruiz de Almodovar, C. Neurovascular Communication during CNS Development. *Dev Cell* **45**, 10-32, doi:10.1016/j.devcel.2018.01.023 (2018).
14 Himmels, P. et al. Motor neurons control blood vessel patterning in the developing spinal cord. *Nat Commun* **8**, 14583, doi:10.1038/ncomms14583 (2017).
15 Takahashi, T. et al. Angiogenesis in the developing spinal cord: blood vessel exclusion from neural progenitor region is mediated by VEGF and its antagonists. *PloS one* **10**, e0116119, doi:10.1371/journal.pone.0116119 (2015).
16 James, J. M., Gewolb, C. & Bautch, V. L. Neurovascular development uses VEGF-A signaling to regulate blood vessel ingression into the neural tube. *Development* **136**, 833-841, doi:10.1242/dev.028845 (2009).
17 Walchli, T. et al. Wiring the Vascular Network with Neural Cues: A CNS Perspective. *Neuron* **87**, 271-296, doi:10.1016/j.neuron.2015.06.038 (2015).
18 Augustin, H. G. & Koh, G. Y. Organotypic vasculature: From descriptive heterogeneity to functional pathophysiology. *Science* **357**, eaal2379, doi:10.1126/science.aal2379 (2017).
19 Rafii, S., Butler, J. M. & Ding, B. S. Angiocrine functions of organ-specific endothelial cells. *Nature* **529**, 316-325, doi:10.1038/nature17040 (2016).
20 Ramasamy, S. K., Kusumbe, A. P. & Adams, R. H. Regulation of

tissue morphogenesis by endothelial cell-derived signals. *Trends Cell Biol* **25**, 148-157, doi:10.1016/j.tcb.2014.11.007 (2015).
21 Augustin, H. G., Koh, G. Y., Thurston, G. & Alitalo, K. Control of vascular morphogenesis and homeostasis through the angiopoietin-Tie system. *Nat Rev Mol Cell Biol* **10**, 165-177, doi:10.1038/nrm2639 (2009).
22 Hu, J. et al. Endothelial cell-derived angiopoietin-2 controls liver regeneration as a spatiotemporal rheostat. *Science* **343**, 416-419, doi:10.1126/science.1244880 (2014).
23 Fagiani, E. & Christofori, G. Angiopoietins in angiogenesis. *Cancer Lett* **328**, 18-26, doi:10.1016/j.canlet.2012.08.018 (2013).
24 Tekki-Kessaris, N. et al. Hedgehog-dependent oligodendrocyte lineage specification in the telencephalon. *Development* **128**, 2545-2554 (2001).
25 Li, Y. et al. Sonic hedgehog (Shh) regulates the expression of angiogenic growth factors in oxygen-glucose-deprived astrocytes by mediating the nuclear receptor NR2F2. *Mol Neurobiol* **47**, 967-975, doi:10.1007/s12035-013-8395-9 (2013).
26 Pola, R. et al. The morphogen Sonic hedgehog is an indirect angiogenic agent upregulating two families of angiogenic growth factors. *Nat Med* **7**, 706-711, doi:10.1038/89083 (2001).
27 Yam, P. T., Langlois, S. D., Morin, S. & Charron, F. Sonic hedgehog guides axons through a noncanonical, Src-family-kinase-dependent signaling pathway. *Neuron* **62**, 349-362, doi:S0896-6273(09)00247-5 [pii]
10.1016/j.neuron.2009.03.022 (2009).
28 Langlois, S. D., Morin, S., Yam, P. T. & Charron, F. Dissection and culture of commissural neurons from embryonic spinal cord. *J Vis Exp*, doi:10.3791/1773 (2010).
29 Agius, E. et al. Converse control of oligodendrocyte and astrocyte lineage development by Sonic hedgehog in the chick spinal cord. *Dev Biol* **270**, 308-321, doi:10.1016/j.ydbio.2004.02.015 (2004).
30 Bergles, D. E. & Richardson, W. D. Oligodendrocyte Development and Plasticity. *Cold Spring Harb Perspect Biol* **8**, a020453, doi:10.1101/cshperspect.a020453 (2015).
31 Touahri, Y. et al. Sulfatase 1 promotes the motor neuron-to-oligodendrocyte fate switch by activating Shh signaling in Olig2 progenitors of the embryonic ventral spinal cord. *J Neurosci* **32**, 18018-18034, doi:10.1523/JNEUROSCI.3553-12.2012 (2012).
32 Sato, T. N. et al. Distinct roles of the receptor tyrosine kinases Tie-1 and Tie-2 in blood vessel formation. *Nature* **376**, 70-74, doi:10.1038/376070a0 (1995).
33 Jeansson, M. et al. Angiopoietin-1 is essential in mouse vasculature during development and in response to injury. *J Clin Invest* **121**, 2278-2289, doi:10.1172/JCI46322 (2011).
34 Kim, K. H., Nakaoka, Y., Augustin, H. G. & Koh, G. Y. Myocardial Angiopoietin-1 Controls Atrial Chamber Morphogenesis by Spatiotemporal Degradation of Cardiac *Jelly*. *Cell Rep* **23**, 2455-2466, doi:10.1016/j.celrep.2018.04.080 (2018).
35 Tronche, F. et al. Disruption of the glucocorticoid receptor gene in the nervous system results in reduced anxiety. *Nat Genet* **23**, 99-103, doi:10.1038/12703 (1999).
36 Dessaud, E. et al. Interpretation of the sonic hedgehog morphogen gradient by a temporal adaptation mechanism. *Nature* **450**, 717-720, doi:10.1038/nature06347 (2007).
37 Motoike, T. et al. Universal GFP reporter for the study of vascular development. *Genesis* **28**, 75-81 (2000).
38 Savant, S. et al. The Orphan Receptor Tie1 Controls Angiogenesis and Vascular Remodeling by Differentially Regulating Tie2 in Tip and Stalk Cells. *Cell Rep* **12**, 1761-1773, doi:10.1016/j.celrep.2015.08.024 (2015).
39 Palazuelos, J., Klingener, M. & Aguirre, A. TGFbeta signaling regulates the timing of CNS myelination by modulating oligodendrocyte progenitor cell cycle exit through SMAD3/4/FoxO1/Sp1. *J Neurosci* **34**, 7917-7930, doi:10.1523/JNEUROSCI.0363-14.2014 (2014).
40 Massague, J. TGFbeta signalling in context. *Nat Rev Mol Cell Biol* **13**, 616-630, doi:10.1038/nrm3434 (2012).
41 Dessaud, E., McMahon, A. P. & Briscoe, J. Pattern formation in the vertebrate neural tube: a sonic hedgehog morphogen-regulated transcriptional network. *Development* **135**, 2489-2503, doi:10.1242/dev.009324 (2008).
42 Tsai, H. H. et al. Oligodendrocyte precursors migrate along vasculature in the developing nervous system. *Science* **351**, 379-384, doi:10.1126/science.aad3839 (2016).
43 Yuen, T. J. et al. Oligodendrocyte-encoded HIF function couples postnatal myelination and white matter angiogenesis. *Cell* **158**, 383-396, doi:10.1016/j.cell.2014.04.052 (2014).

Curriculum Vitae
Isidora Paredes Ugarte, Dr. rer. nat.

Place of birth: Santiago de Chile, Chile
Nationality: Chile
Address: Vascular Dysfunction Department, European Center for Angioscience, Medical Faculty Mannheim, Heidelberg University, Ludolph-Krehl Str. 13-17, 68167 Mannheim, Germany
e-mail: isidora.paredesugarte@medma.uni-heidelberg.de

Education

2013 – 2019 **Dr. rer. nat. in Biology**, Biochemistry Center, Heidelberg University, Heidelberg, Germany.
2010 – 2012 **Biochemistry Diploma**, Pontifical Catholic University of Chile, Santiago, Chile.
2005 – 2010 **Bachelor and Licentiate in Biochemistry**, Pontifical Catholic University of Chile, Santiago, Chile.

Research Experience

2019 – 2021 **Postdoctoral fellow.** Vascular Dysfunction department, Prof. Dr. Carmen Ruiz de Almodóvar, European Center for Angioscience, Medical Faculty Mannheim, Heidelberg University, Mannheim, Germany.
2013 – 2019 **Ph.D. student in Natural Sciences.** Biochemistry Center, Dr. Ruiz de Almodóvar, Heidelberg University, Heidelberg, Germany.
2011 – 2012 **Undergraduate research fellow.** Cell and Molecular Biology department, Dr. Erices, Pontifical Catholic University of Chile, Santiago, Chile.

Fellowships, Scholarships and Awards

2021 **Werner Risau prize.** German Society of Cell Biology, DGZ, Germany
2021 **EVBO publication highlight** winner March 2021, European Vascular Biology Organization
2018 **Best poster prize** EMBO Workshop-Neurodevelopment, Taipei, Taiwan
2018 **EMBO travel award**
2012 – 2016 **Ph.D. fellowship** BECAS Chile - Chilean Scientific Agency
2012 **DAAD Summer School** fellow, Berlin Brandenburg School for regenerative Therapies, Charité Universitätsmedizin, Berlin, Germany
2005 – 2011 **Bachelor and Diploma studies scholarship** Las Condes municipality, Santiago, Chile

Research interest and activity

During my diploma in Biochemistry at the Catholic University of Chile in Santiago, Chile, I was first introduced to endothelial cell biology and got fascinated by the fact that blood vessels are not silent bystanders rather their signaling is needed for an endless number of processes. I got particularly interested in neurovascular interactions and carried out a thesis focusing on the role of angiogenic factors secreted by bone marrow mesenchymal stromal cells in regulating embryonic neural stem cells properties. Afterwards, I obtained a fellowship for my doctorate studies and joined Prof. Ruiz de Almodóvar lab for my Ph.D. and later a Postdoc. Here, I got deeply interested in understanding how the neurovascular crosstalk drives central nervous system development and contributed to studies uncovering how developing motor neurons control blood vessel patterning (*Nat. Comm., 2017*) and how cell-death signaling pathways contribute to vascular development in embryos (*JCI, 2019*). During my Ph.D. studies and Postoctoral research I was interested in understanding how blood vessels could instruct cell fate specification during CNS development. Research of the past decades has shown that vessels are crucial active regulators of tissue formation, organ function, and regeneration. However, little is known about the active angiocrine role the vasculature has in the CNS. My research addressed these questions by describing a unique bidirectional molecular crosstalk in the developing CNS where blood vessels coordinate neural progenitor cells to guide CNS development (*Nat. Neuroscience, 2021- Werner Risau Prize*). The novelty of this study relies not only on the original findings describing for the first time a functional active bi-directional communication in vivo via neural-derived Angiopoitin1 signaling to endothelial-Tie2 activation and angiocrine Tgfβ1 signaling axis necessary for oligodendrocyte precursor cell specification, but also these findings integrate building blocks from different cellular compartments in the neurogenic niche, and how they coordinate converging in the instruction and control of oligodendrogenesis. Moreover, I found that lack of this signaling axis results in delayed myelination. Impaired oligodendrocyte generation and function are key features of many diseases, such as multiple sclerosis in adults or periventricular leukomalacia, a typical dysmyelinating disorder in premature infants. For my next career steps, I am particularly intrigued by understanding interdependent molecular interactions between the vasculature and neurons and other non-vascular cells within different niche environments and how molecular cross talks are crucial in physiological and pathological conditions.

Publications

1. **Paredes, I.**, Vieira, J. R., Shah, Ramunno CF, Dyckow J, Adler H, Richter M, Schermann G, Giannakouri E, Schirmer L, Augustin HG, and Ruiz de Almodóvar, C. (2021). Oligodendrocyte precursor cell specification is regulated by bidirectional neural progenitor–endothelial cell crosstalk. *Nature Neuroscience*, *24* (April). https://doi.org/10.1038/s41593-020-00788-z
2. Tisch, N.*, Freire-Valls, A.*, Yerbes, R.*, **Paredes, I.**, La Porta S, Wang X, Martín-Pérez R, Castro L, Wong WW, Coultas L, Strilic B, Gröne HJ, Hielscher T, Mogler C, Adams RH, Heiduschka P, Claesson-Welsh L, Mazzone M, López-Rivas A, Schmidt T, Augustin HG, and Ruiz De Almodóvar, C. (2019). Caspase-8 modulates physiological and pathological angiogenesis during retina development. *Journal of Clinical Investigation*, *129(12)*, 5092–5107. https://doi.org/10.1172/JCI122767
3. **Paredes, I.**, Himmels, P., and Ruiz de Almodóvar, C. (2018). Neurovascular Communication during CNS Development. *Developmental Cell 45(1)*, 10-32. https://doi.org/10.1016/j.devcel.2018.01.023
4. Himmels, P., **Paredes, I.**, Adler, H., Karakatsani, A., Luck, R., Marti, H. H., Ermakova, O., Rempel, E., Stoeckli, E.T., Ruiz de Almodóvar, C. (2017). Motor neurons control blood vessel patterning in the developing spinal cord. *Nature Communications, 8* (March 2017), 14583. https://doi.org/10.1038/ncomms14583

"Liquid Organelles"

Meeting report of the 19th Workshop "Cell Biology of Viral Infections" of the German Society of Virology (GfV) in Schöntal, October 20th–22nd, 2021.

By Thomas Hoenen[1] and Eva Herker[2]

Group photo with 2021 workshop participants in front of the main building of the Cistercian Monastery Schöntal.

This year, the Workshop "Cell Biology of Viral Infection" of the German Society of Virology (GfV) was focused on Liquid Organelles. The lectures of the four keynote speakers of the 2021 meeting perfectly illustrated different aspects of principles of liquid-liquid phase separation, ranging from biophysical principles to disease-related processes and viral replication organelle formation.

In 2020, Dr. Thomas Hoenen (Friedrich-Loeffler-Institute) and Dr. Eva Herker (Philipps-University Marburg) took over organizing the annual workshop. Due to the SARS-CoV-2 pandemic, the 2020 meeting on Liquid Organelles had to be postponed. It now took place from October 20th to 22nd 2021 as an in-person meeting, following 2G rules of Baden-Württemberg, at the Monastery Schöntal, Germany. We were very pleased that almost all

[1] Friedrich-Loeffler-Institut, Federal Research Institute for Animal Health, Südufer 10, 17493 Greifswald - Insel Riems, Germany
[2] Institute of Virology, Philipps University Marburg, Hans-Meerwein-Strasse 2, 35043 Marburg, Germany

participants were able to directly stay at the conference site, which stimulated active discussions during the poster session, lunch and dinner gatherings, as well as at the social events.
The theme of this year was "Liquid Organelles", an emerging field in cell biological research that is key to replication of many negative-stranded RNA viruses and likely beyond. The program included four keynote lectures, 24 oral presentations, and a poster session. The workshop resonance was again great with 48 on-site participants, including among others 38 students and post-docs.
The majority of the participants were virologists from Germany, but also scientists from Switzerland, Poland, France and Portugal attended the meeting. The four excellent keynote speakers from the Netherlands, Switzerland, France, and Italy, as well as the enthusiastic participants significantly contributed to the success of the workshop. Noteworthy was the active participation of students and postdocs in the discussions during and after the sessions.
The workshop opened with the exciting keynote lecture "Phase separated compartments in the nucleus and protein quality control" given by Dr. Mark Steffen Hipp from the University of Groningen, Netherlands. His research focusses on the investigation of toxic effects of protein aggregates in phase-separated compartments in the nucleus and the interactions of multiple different disease-associated proteins with the cellular quality control machinery, highlighting the impact of phase separation on neurological disorders.
Dr. Yves Gaudin from CNRS, Institut de Biologie Intégrative de la Cellule in Gif sur Yvette, France, underscored the importance of liquid-liquid phase separation for the formation of replication organelles, in this case of rabies virus, a negative-stranded RNA virus. The research he presented focused on the exciting interplay between viral factories and innate immunity during rabies virus infection.
The third insightful keynote lecture presented by Dr. Monika Fuxreiter from the University of Padova, Italy, illustrated the biophysical principles that guide the formation of liquid organelles as well as protein interactions within these condensates. Her work also illustrated the utility of computational tools and in vitro studies to elucidate the role of conformational states of proteins in condensation.
Finally, Dr. Lucas Pelkmans from the University of Zurich, Switzerland, presented his exciting work on DYRK kinases, which act as regulators of intracellular condensate formation. His work revealed cellular signaling pathways that can be manipulated to control the formation of liquid organelles.
Among the many excellent presentations from junior scientists, the audience voted on the prize winner for the best oral presentation. Sophie Winter from Petr Chlanda's group at the University of Heidelberg, Germany, was awarded the prize for the best oral presentation for her work entitled "Cryo-electron tomography reveals Ebola virus uncoating at low pH".
As in previous years, the workshop featured a poster session in addition to the oral presentations. This year, the two keynote speakers Yves Gaudin and Mark Steffen Hipp had the difficult task to pick the best poster presentation. Georgios Vavouras Syrigos from Michael Schindler's lab at the University of Tübingen, Germany, was selected for his work on "Regulation of SAMHD1 upon HCMV infection and potential of CDK4/6 inhibitors to suppress HCMV replication in macrophages".
According to immediate feedback from participants, the fact that the meeting took place as an in-person workshop was highly appreciated. Students, postdocs, and PIs lauded the exciting contents and quality of the keynote lectures. Everyone praised the high quality of all presentations and the friendly and engaging atmosphere in which the meeting took place.
The organizers would like to thank the German Society for Virology (GfV), the German Society for Cell Biology (DGZ), and the company ReBlikon for their support. The workshop would not have been possible without these generous contributions.
The date, topic, and venue for the next workshop are already decided on: The 20th Workshop "Cell Biology of Viral Infection" of the German Society of Virology (GfV) will take place from October 12th to 14th 2022 at the Monastery Schöntal. The exciting topic will be "Organoids". More information and updates can be found on the workshop's website:
https://cellviro.g-f-v.org/

Photos of the winners of the prize for the best oral (left) and poster (right) presentation of the 2021 workshop.

Life at the edge: The nuclear envelope and nucleocytoplasmic transport

International Meeting of the German Society for Cell Biology (DGZ)

CONFIRMED SPEAKERS

Alwin Köhler
Vienna
Abby Buchwalter
San Francisco
Andre Hoelz
Pasadena
Anita Corbett
Atlanta
Christian Schlieker
New Haven
David Jans
Monash
Dirk Görlich
Göttingen
Patrick Lusk
New Haven
Rod Lim
Basel
Rose Goodchild
Leuven
Susan Gasser
Lausanne
Thomas Schwartz
Boston
Wendy Bickmore
Edinburgh
Valerie Doye
Paris
Dorothee Dormann
Mainz
Edward Lemke
Mainz
Eric Schirmer
Edinburgh
Jeff Rothstein
Baltimore
Karsten Weis
Zürich
Larry Gerace
La Jolla
Liesbeth Veenhoff
Groningen
Mark Field
Dundee
Martin Beck
Frankfurt
Mary Dasso
Bethesda
Maxi D'Angelo
La Jolla
Maya Capelson
Philadelphia
Megan King
New Haven
Mike Rout
New York
Naoko Imamoto
Hirosawa
Yaron Shav-Tal
Ramat Gan
Yuh Min Chook
Dallas

Potsdam, July 20-24, 2022

Kongresshotel, Potsdam

ORGANIZERS

Birthe Fahrenkrog
University of Basel
Birthe.Fahrenkrog@unibas.ch

Ralph Kehlenbach
University of Göttingen
rkehlen@gwdg.de

REGISTRATION and ABSTRACTS
https://zellbiologie.de/en/meetings/
DEADLINE: APRIL 20, 2022

additional speakers will be selected from the abstracts

picture by Ralph Graf, Potsdam

Impressum

Publisher:
Deutsche Gesellschaft für
Zellbiologie e.V. (DGZ)
(German Society for Cell Biology)

Editor-in-Chief:
Prof. Dr. Roland Wedlich-Söldner,
Präsident (Universität Münster)

Editors:
Prof. Dr. Gislene Pereira
(Universität Heidelberg)
Prof. Dr. Sandra Iden
(Universität des Saarlandes)
Ralf Jungmann
(Universität München und
Max Planck Institut für Biochemie)
Prof. Dr. Ludwig Eichinger
(Universität zu Köln)
Prof. Dr. Friedemann Kiefer
(MPI Molekulare Biomedizin, Münster)

Editorial Office
Manuscripts/Advertisements:
Sabine Reichel-Klingmann
Office of the German Society
for Cell Biology
c/o German Cancer Research Center
Im Neuenheimer Feld 280
69120 Heidelberg
Tel.: 06221/42-3451
Fax: 06221/42-3452
E-mail: dgz@dkfz.de
Internet: www.zellbiologie.de

Production:
abcdruck GmbH
Waldhofer Str. 19 · 69123 Heidelberg
info@abcdruck.de · www.abcdruck.de

Media Creation:
Thomas Weber
t.weber@abcdruck.de

Full electronic version

Frequency of publication:
3-4 issues yearly

If you are interested in advertising, please contact the DGZ office (dgz@dkfz.de)

Privacy Policy:
https://zellbiologie.de/datenschutz/